Article

# RNA N-glycosylation enables immune evasion and homeostatic efferocytosis

https://doi.org/10.1038/s41586-025-09310-6

Received: 5 June 2024

Accepted: 19 June 2025

Published online: 6 August 2025

Check for updates

Vincent R. Graziano[1], Jennifer Porat[2], Marie Dominique Ah Kioon[3], Ivana Mejdrová[4], Alyssa J. Matz[1], Charlotta G. Lebedenko[2], Peiyuan Chai[2], John V. Pluvinage[5,6], Rafael Ricci-Azevedo[1], Andrew G. Harrison[1], Skylar S. Wright[1], Xinzheng Wang[1], Madison S. Strine[7], Penghua Wang[1], Michael R. Wilson[5,6], Sivapriya Kailasan Vanaja[1], Beiyan Zhou[1,8], Franck J. Barrat[3,9], Thomas Carell[4], Ryan A. Flynn[2,10,11,12] ✉ & Vijay A. Rathinam[1,12] ✉

Glycosylation is central to the localization and function of biomolecules[1]. We recently discovered that small RNAs undergo N-glycosylation[2] at the modified RNA base 3-(3-amino-3-carboxypropyl) uridine (acp$^3$U)[3]. However, the functional significance of N-glycosylation of RNAs is unknown. Here we show that the N-glycans on glycoRNAs prevent innate immune sensing of endogenous small RNAs. We found that de-N-glycosylation of cell-culture-derived and circulating human and mouse glycoRNA elicited potent inflammatory responses including the production of type I interferons in a Toll-like receptor 3- and Toll-like receptor 7-dependent manner. Furthermore, we show that N-glycans on cell surface RNAs prevent apoptotic cells from triggering endosomal RNA sensors in efferocytes, thus facilitating the non-inflammatory clearance of dead cells. Mechanistically, N-glycans conceal the hypermodified uracil base acp$^3$U, which we identified as immunostimulatory when exposed in RNA. Consistent with this, genetic deletion of an enzyme (DTWD2) that synthesizes acp$^3$U abrogated innate immune activation by de-N-glycosylated small RNAs and apoptotic cells. Furthermore, synthetic acp$^3$U-containing RNAs are sufficient to trigger innate immune responses. Thus, our study has uncovered a natural mechanism by which N-glycans block RNAs from inducing acp$^3$U-dependent innate immune activation, demonstrating how glycoRNAs exist on the cell surface and in the endosomal network without inducing autoinflammatory responses.

RNA sensing is a critical innate immune surveillance programme that protects the host from invading pathogens. Pattern recognition receptors (PRRs) monitor the endosomes and cytosol for foreign RNA. In the endosomal compartment, Toll-like receptor 3 (TLR3) senses double-stranded RNA (dsRNA), whereas TLR7 and TLR8 sense single-stranded RNA (ssRNA)[4–8]. RIG-I-like receptors, retinoic-acid inducible gene-I and melanoma differentiation-associated protein 5 survey for foreign RNA in the cytosol[9,10]. Consequently, RNA sensing by TLRs and RIG-I-like receptors stimulates innate immune responses, such as NF-κB-dependent expression of pro-inflammatory cytokines and interferon regulatory factor 3 or 7 (IRF3 or IRF7)-dependent expression of type I interferons[11–13]. As RNA is not a pathogen-specific molecular pattern, the host deploys numerous mechanisms to prevent immune sensing of self-RNA. These mechanisms include the spatial exclusion of RNA sensors from self-RNA, the expression of RNases to limit ligand availability to RNA sensors and self-RNA modifications.

N-glycosylation is a recently identified RNA modification. Diverse small non-coding RNAs including transfer RNAs (tRNAs), Y RNAs, small nuclear RNAs (snRNAs) and small nucleolar RNAs (snoRNAs) are modified with sialic acid-containing N-linked glycans (glycoRNAs)[2]. A direct site for N-glycosylation on RNA has been characterized at 3-(3-amino-3-carboxypropyl) uridine (acp$^3$U)[3], which is predominantly found in the D-loop of eukaryotic tRNA[14]. GlycoRNAs are proposed to be trafficked into the endoplasmic reticulum for N-glycosylation, guided to the cell surface through the endoplasmic reticulum–Golgi network, deployed on the cell surface and presumably constitutively endocytosed without stimulating immune sensors[2,15,16]. However, the mechanisms preventing self-sensing of glycoRNAs and the functional importance of RNA glycosylation remain unknown. Furthermore, the cell surface localization of glycoRNA poses a challenge for the immunologically silent removal of dead cells. Apoptotic cells are cleared mostly by tissue-resident macrophages by means of efferocytosis, mediated

[1]Department of Immunology, UConn Health School of Medicine, Farmington, CT, USA. [2]Stem Cell Program and Division of Hematology/Oncology, Boston Children's Hospital, Boston, MA, USA. [3]HSS Research Institute and David Z. Rosensweig Genomics Research Center, Hospital for Special Surgery, New York, NY, USA. [4]Department of Chemistry, Institute of Chemical Epigenetics—Munich (ICE-M), Ludwig-Maximilians-Universität (LMU) München, Munich, Germany. [5]Department of Neurology, University of California, San Francisco (UCSF), San Francisco, CA, USA. [6]Weill Institute for Neurosciences, UCSF, San Francisco, CA, USA. [7]Department of Immunobiology, Yale School of Medicine, New Haven, CT, USA. [8]Institute for Systems Genomics, University of Connecticut, Farmington, CT, USA. [9]Department of Microbiology and Immunology, Weill Cornell Medical College of Cornell University, New York, NY, USA. [10]Department of Stem Cell and Regenerative Biology, Harvard University, Cambridge, MA, USA. [11]Harvard Stem Cell Institute, Harvard University, Cambridge, MA, USA. [12]These authors contributed equally: Ryan A. Flynn, Vijay A. Rathinam. ✉e-mail: Ryan.Flynn@childrens.harvard.edu; Rathinam@uchc.edu

by phagocytic receptor recognition of eat-me ligands on dead cells[17]. A key feature of efferocytosis is that it occurs without eliciting inflammation. In this context, cell surface-exposed glycoRNA risks activation of endosomal RNA receptors when cells become apoptotic and engulfed by phagocytes[18]. However, the molecular mechanism that prevents the sensing of glycoRNAs during efferocytosis, enabling homeostatic efferocytosis, is not known.

In this study, we provide evidence that the N-glycosylation of endogenous small RNAs prevents their detection by innate immune PRRs. We found that enzymatic removal of N-glycans from RNAs stimulates RNA-sensing pathways leading to a potent type I interferon response. Consistent with this finding, removing N-glycans from apoptotic cells induced an inflammatory response in an RNA-dependent manner upon efferocytosis by macrophages. Our studies show that acp$^3$U, a linker between N-glycans and RNA that gets exposed upon de-N-glycosylation, renders RNA immunostimulatory. Finally, both TLR3 and TLR7 sense acp$^3$U-containing de-N-glycosylated RNA in macrophages. Altogether, this study shows that by caging acp$^3$U, N-glycosylation of RNAs deters innate immune sensing of self-RNAs, facilitating the non-inflammatory clearance of dead cells.

## RNA N-glycans prevent immune activation

To investigate whether N-glycosylation of RNA serves as a determinant of self- versus non-self-nucleic acid sensing, we isolated the small RNA fraction from HeLa cells (enriched for sialoglycoRNAs)[2,19] and treated with enzymes that cleave N-glycans (PNGase F) and RNA (RNase cocktail: RNase A, RNase T1 and RNase III, referred to as RNase hereafter) individually and in combination[2,20]. After enzymatic digestion, we transfected these RNAs into RAW macrophages and assessed the production of interferon-β (IFNβ), the signature outcome of nucleic acid sensing (Extended Data Fig. 1a). We observed no induction of IFNβ in our lipofectamine controls or upon transfection of native small RNA at two different concentrations (Fig. 1a). However, small RNAs de-N-glycosylated with PNGase F induced robust IFNβ production. Pretreatment of PNGase F-treated small RNA with RNase abolished IFNβ production attributing the interferon response to intact, but de-N-glycosylated RNA (Fig. 1a). We also observed that de-N-glycosylated small RNA was able to induce IFNβ expression when added to RAW macrophages without transfection (Extended Data Fig. 1b). Thus, removing N-glycans with PNGase F from small RNA elicits IFNβ production. By contrast, PNGase F treatment did not confer an immunostimulatory activity to long RNA, which do not contain glycoRNAs[2,19] (Fig. 1b). PNGase F also had no effect on IFNβ induction by poly(I:C), a synthetic RNA that has no glycans (Fig. 1c). These data show de-N-glycosylation of small RNAs as a potent inducer of type I interferons.

We next examined the activation of TANK-binding kinase 1 (TBK1) and interferon regulatory factor 3 (IRF3), key components of PRR signalling that drive type I interferon production[21]. We observed phosphorylation of TBK1 (pTBK1) and IRF3 (pIRF3) only in cells transfected with PNGase F-treated small RNAs (Fig. 1d). We also assessed the phosphorylation of JNK, ERK1/2 and p38, as well as NF-κB p65—components of innate immune signalling—by immunoblotting and found that PNGase F-treated small RNAs stimulated the activation of JNK, ERK1/2, p38 and NF-κB p65 in RAW macrophages (Fig. 1e). Furthermore, de-N-glycosylated RNA induced assembly of the myddosome—a central upstream event in the TLR signalling[22]—albeit weakly compared to the synthetic TLR2 agonist Pam3CSK4 (Extended Data Fig. 1c). The immunostimulatory effect of de-N-glycosylated small RNA was not limited to RAW macrophages, as mouse peritoneal macrophages as well as primary human plasmacytoid dendritic cells (pDCs) and macrophages also robustly produced type I interferons, tumour necrosis factor (TNF) and/or interleukin-6 (IL-6) upon stimulation with PNGase F-treated small RNA (Fig. 1f and Extended Data Fig. 1d,e). These data reveal that de-N-glycosylated small RNAs activate innate immune signalling.

Because of the constitutive endocytic process, cell surface glycoRNAs continuously localize in the endosomes containing RNA sensors. In this context, we hypothesized that de-N-glycosylation of cell surface glycoRNAs by adding large amounts of PNGase F directly to cells would stimulate RNA sensors in the endosome, in *cis*, as cells constitutively endocytose cell surface components. To test this, we added increasing doses of PNGase F (3, 9 and 15 times the amount used to treat isolated small RNA samples in our previous experiments) or PNGase F and RNase to RAW macrophages. We note that even adding three times the amount of PNGase F (2 μg) used to treat purified small RNA fractions to cells did not induce a robust interferon production (Extended Data Fig. 1f). By contrast, adding nine times more PNGase F to macrophages induced an RNA-dependent innate immune response (Extended Data Fig. 1f). These data are supportive of a model in which cells present RNAs on their surface that are normally N-glycosylated and, thus, invisible to RNA sensors upon constitutive endocytosis. Overall, our data indicate that glycoRNAs are shielded by their N-glycans from innate immune RNA sensors.

## Deglycosylated serum RNA is stimulatory

Whereas glycoRNAs were first described to exist on the cell surface, small RNAs have been found in the peripheral blood of vertebrates[23,24]. We thus asked whether mouse and human blood also contains sialoglycoRNAs. We isolated RNAs from mouse and human sera as well as from HeLa cells (the latter for comparison) and labelled them with rPAL: a periodate oxidation and aldehyde ligation method to detect native sialoglycoRNAs[3]. We observed rPAL signals in all three sources. Comparative analysis of rPAL-labelled cell- and sera-isolated RNA demonstrated that the sialoglycoRNA to total RNA ratio was higher in human and mouse sera-isolated RNA compared to the cell-isolated RNA and revealed different molecular weight banding patterns (Fig. 1g and Extended Data Fig. 2a,b). Normalizing for the amount of RNA labelled (1 μg, quantified before rPAL labelling as sera-isolated RNA was not visible in the gel), sera RNA generated 38-fold more rPAL signal than HeLa cell RNA per μg of RNA (Extended Data Fig. 2c–e). Having identified glycoRNAs in circulation, we next asked whether sera glycoRNA is similarly immunogenic upon de-N-glycosylation with PNGase F. We found that de-N-glycosylated mouse and human sera RNA potently induced the production of IFNβ, TNF and IL-6 when compared to untreated sera RNA in mouse peritoneal macrophages and human THP1 macrophages (Fig. 1h–k). As we found with cellular small RNA, RNase treatment of de-N-glycosylated sera-derived RNAs blunted its immunostimulatory activity (Fig. 1h–k). Considering the link between aberrant sensing of endogenous RNAs[25–28] and anti-dsRNA antibodies and autoimmune diseases such as systemic lupus erythematosus (SLE)[29], we assessed whether there were alterations in circulating sialoglycoRNA in a small set of healthy controls and patients with SLE. We subjected the isolated RNA to rPAL analysis and found heterogeneity in sera-isolated sialoglycoRNA signals across individuals (Extended Data Fig. 2f). Whereas the two highest intensity samples are from patients with SLE, the overall changes are not statistically significant (Extended Data Fig. 2f). Overall, these data revealed that glycoRNAs are present in mouse and human circulation and that their de-N-glycosylation elicits inflammatory responses.

## RNA N-glycans aid silent efferocytosis

Efferocytosis of apoptotic cells is a fundamental immunologically silent process that is critical for tissue homeostasis[30]. Having RNA exposed on the cell surface risks activation of endosomal RNA receptors when cells become apoptotic and engulfed by phagocytes. Therefore, we hypothesized that the N-glycans on RNA may prevent the activation of endosomal RNA receptors during efferocytosis. To test this hypothesis, we induced apoptosis in HeLa cells by treating them with

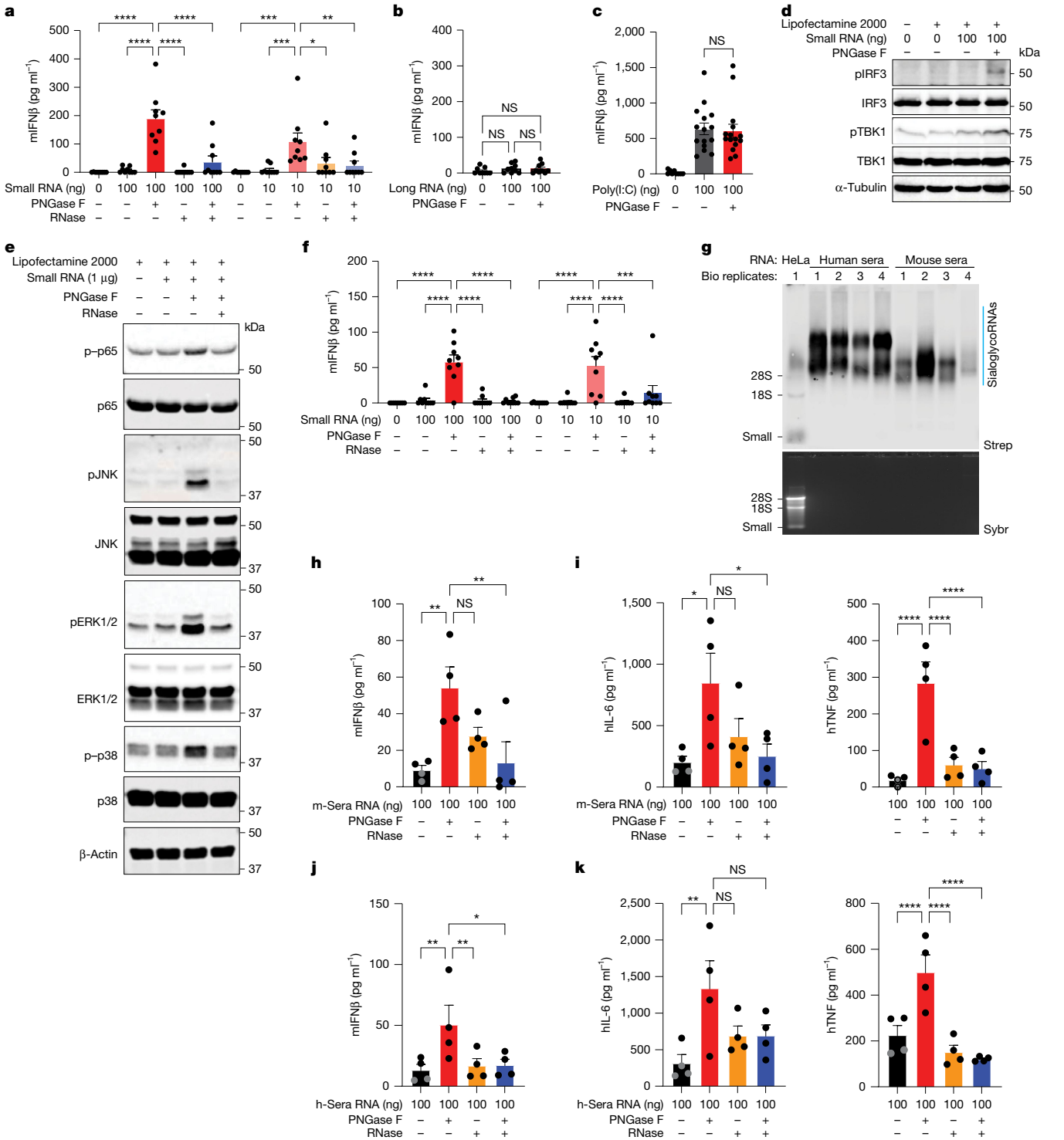


**Fig. 1 | N-glycans shield small RNAs from innate immune recognition.** **a**, IFNβ enzyme-linked immunosorbent assay (ELISA) of RAW macrophage supernatants 6 h posttransfection of small RNA untreated or treated with PNGase F, RNase cocktail or PNGase F + RNase cocktail. **b**, IFNβ ELISA of RAW macrophage supernatants 6 h posttransfection with long RNA treated with or without PNGase F. **c**, IFNβ ELISA of RAW macrophage supernatants 6 h posttransfection with poly(I:C) treated as in **b**. **d**,**e**, Immunoblotting of lysates from RAW macrophages transfected with small RNAs treated with or without PNGase F (**d**) or in combination with RNase (**e**) for different signalling proteins. **f**, IFNβ ELISA of peritoneal macrophage supernatants 6 h posttransfection with small RNA untreated or treated as in **a**. **g**, rPAL-labelled sialoglycoRNAs from sera samples from human and WT mice visualized with streptavidin IR800 (Strep; top) and total RNA (Sybr; bottom). **h**, IFNβ ELISA of peritoneal macrophage supernatants 6 h posttransfection with mouse-sera-derived (m-Sera) small RNAs untreated or treated with PNGase F, RNase cocktail or PNGase F + RNase cocktail. **i**, IL-6 and TNF ELISA of THP1 macrophage supernatants 6 h posttransfection with mouse-sera-derived small RNAs untreated or treated with PNGase F, RNase or PNGase F + RNase. **j**, IFNβ ELISA of peritoneal macrophage supernatants 6 h posttransfection with human-sera-derived (h-Sera) small RNAs untreated or treated as in **a**. **k**, IL-6 and TNF ELISA of THP1 macrophage supernatants stimulated as in **j**. Data are represented as mean ± standard error of the mean (s.e.m.) (**a**–**c**,**f**,**h**–**k**). Pooled data from three independent experiments (**a**–**c**,**f**) or four human and mouse sera samples from three independent replicates (**h**–**k**) or one experiment representative of two (**d**) or three (**e**,**g**) are shown. $^{*}P < 0.05$; $^{**}P < 0.01$; $^{***}P < 0.001$; $^{****}P < 0.0001$; NS, not significant. Two-way analysis of variance (ANOVA) with Tukey's test (**a**,**f**,**h**–**k**) or one-way ANOVA with Šídák's test (**b**,**c**). mIFNβ, mouse IFNβ; hIL-6, human IL-6.

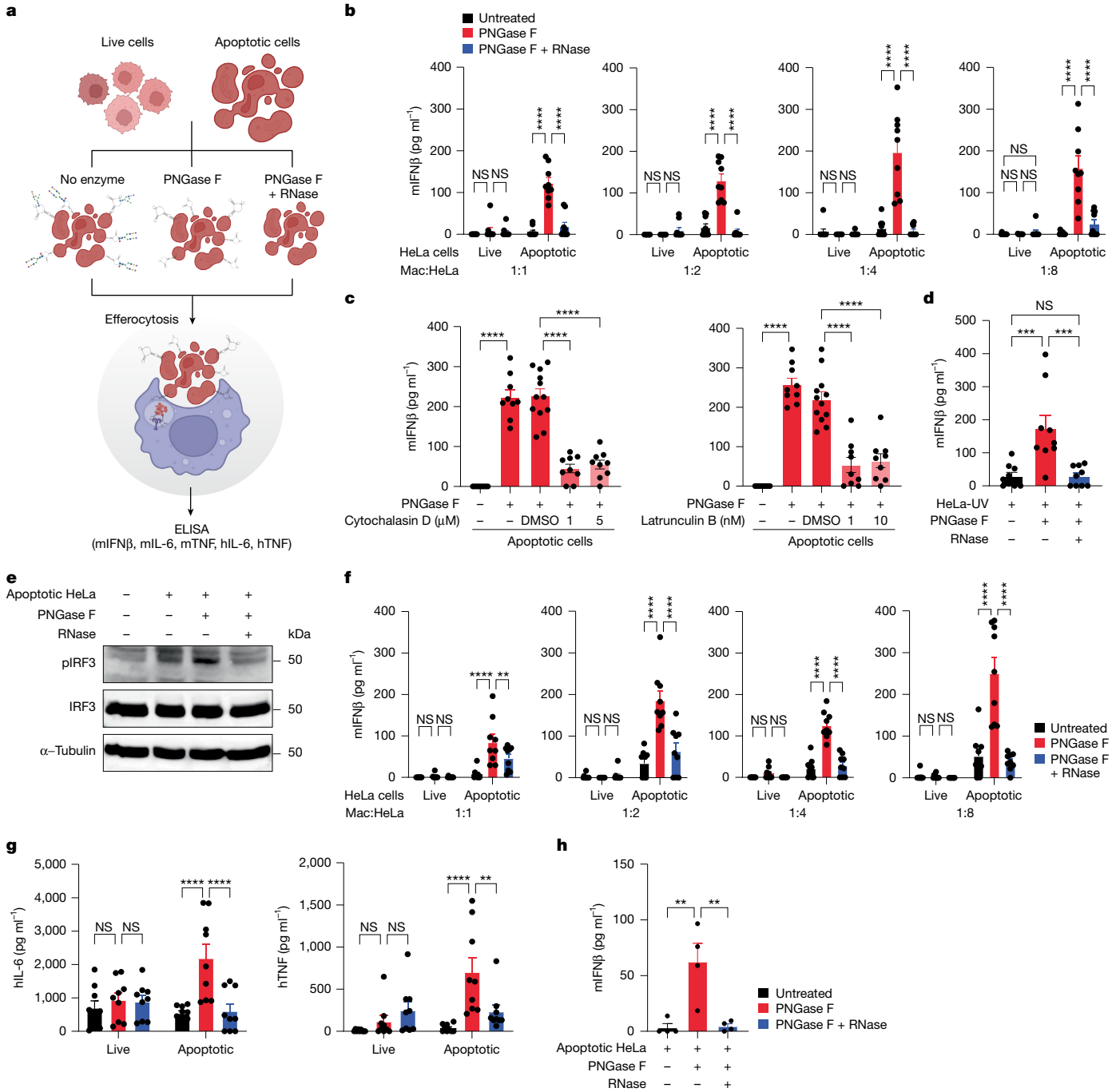


**Fig. 2 | De-N-glycosylation of cell surface RNAs makes apoptotic cells immunostimulatory. a**, Schematic of the experimental design. **b**, IFNβ ELISA of peritoneal macrophage supernatants 24 h poststimulation with live or apoptotic HeLa cells (generated by doxorubicin stimulation) treated with or without PNGase F or PNGase F + RNase at indicated macrophage to HeLa cell ratios (Mac:HeLa). **c**, IFNβ ELISA of supernatants of peritoneal macrophages pretreated with DMSO or with cytochalasin D or latrunculin B for 30 min and stimulated for 24 h with untreated or PNGase F-treated apoptotic cells at a 1:4 macrophage to HeLa cell ratio. **d**, IFNβ ELISA of peritoneal macrophage supernatants 24 h poststimulation with live or apoptotic HeLa cells (generated by ultraviolet light exposure) treated with or without PNGase F or PNGase F + RNase cocktail (1:4 macrophage to HeLa cell ratio). **e**, Immunoblotting of lysates of cells stimulated with untreated, PNGase F-, PNGase F + RNase-treated apoptotic cells for indicated proteins. **f**, IFNβ ELISA of resident peritoneal cell supernatants 24 h poststimulation with live or apoptotic HeLa cells (generated by doxorubicin stimulation) treated with or without PNGase F or PNGase F + RNase cocktail at indicated macrophage to HeLa cell ratios. **g**, IL-6 and TNF ELISA of THP1 macrophage supernatant 24 h poststimulation with live or apoptotic HeLa cells treated with or without PNGase F or PNGase F + RNase cocktail at a 1:4 macrophage to HeLa cell ratio. **h**, IFNβ ELISA of peritoneal lavages from WT mice 24 h after i.p. injection with 10 million apoptotic HeLa cells treated with or without PNGase F or PNGase F + RNase cocktail. Data are represented as mean ± s.e.m. (**b**–**d**,**f**–**h**). Pooled data from three independent experiments (**b**–**d**,**f**–**h**) or one experiment representative of two (**e**) are shown. $^{**}P < 0.01$; $^{***}P < 0.001$; $^{****}P < 0.0001$. Two-way ANOVA with Tukey's test (**b**,**f**,**g**) or one-way ANOVA with Šídák's test (**c**,**d**,**h**). Schematic in **a** was created with BioRender (https://biorender.com).

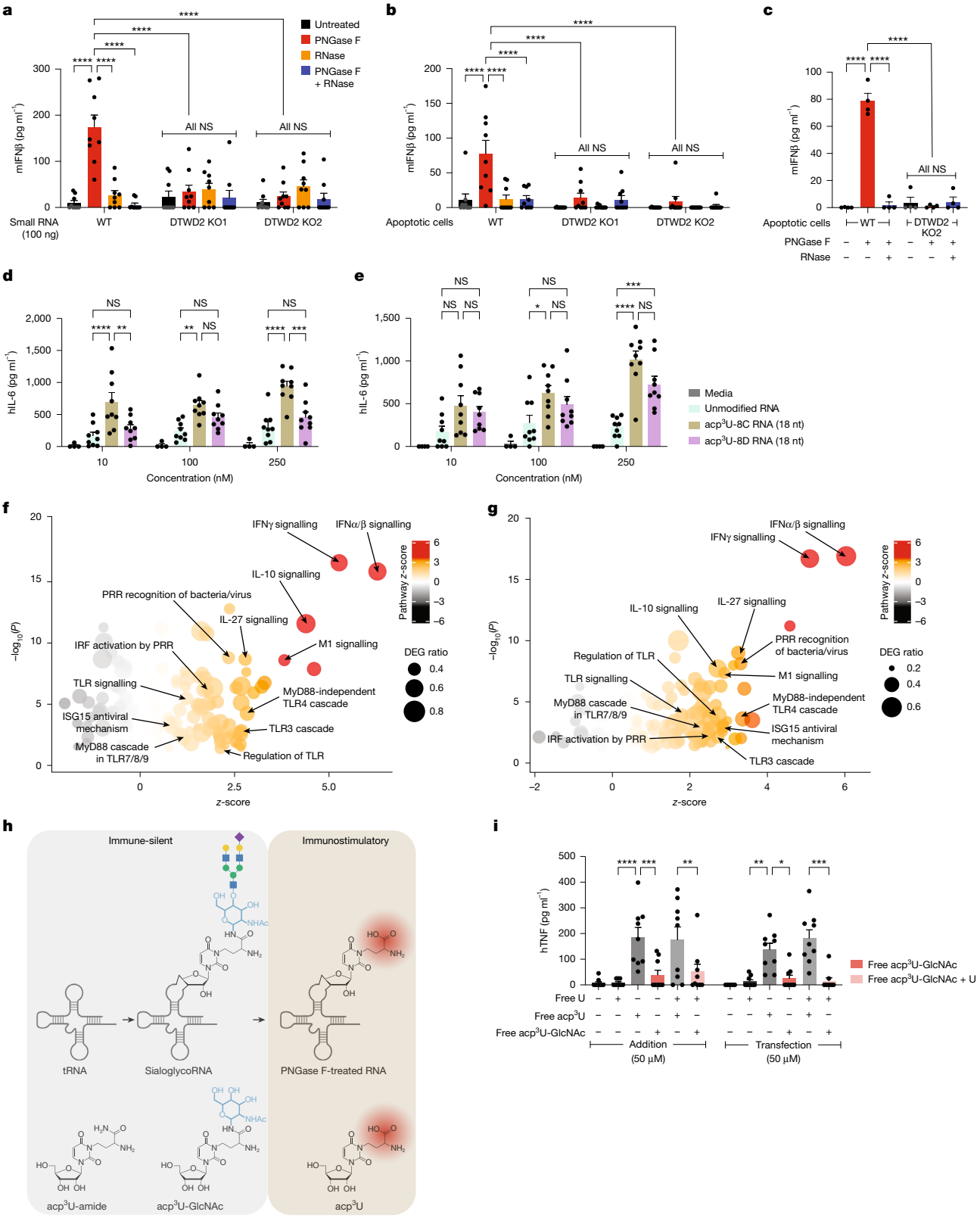


**Fig. 3** | See next page for caption.

doxorubicin[31]. Live and apoptotic cells were subjected to PNGase F treatment to de-N-glycosylate cell surface molecules and then fed to peritoneal macrophages in vitro (Fig. 2a). As expected, control live cells did not induce an inflammatory response even after PNGase F treatment (Fig. 2b). Similarly, apoptotic cells not exposed to PNGase F were non-immunostimulatory. By contrast, we observed a potent induction of IFNβ by apoptotic cells treated with PNGase F, whereas apoptotic cells treated with the combination of PNGase F + RNase induced negligible IFNβ (Fig. 2b). This suggests that the de-N-glycosylation of apoptotic cells induces a potent inflammatory response in an RNA-dependent

**Fig. 3 | RNA containing the modified base acp$^3$U stimulates innate immune responses. a**, IFNβ ELISA of peritoneal macrophage supernatants 6 h posttransfection with small RNA derived from WT and two single cell clones of DTWD2 KO U2OS cells treated with or without PNGase F, RNase cocktail or PNGase F + RNase cocktail. **b**, IFNβ ELISA of peritoneal macrophage supernatants 24 h poststimulation with apoptotic WT, DTWD2 KO1 and DTWD2 KO2 U2OS cells treated with or without PNGase F or PNGase F + RNase cocktail at a 1:4 macrophage to U2OS cell ratio. **c**, IFNβ ELISA of peritoneal lavages from WT mice ($n = 4$) 24 h after i.p. injection with 10 million apoptotic WT or DTWD2 KO U2OS cells treated with or without PNGase F or PNGase F + RNase cocktail. **d**,**e**, IL-6 ELISA of THP1 macrophage supernatants 6 h poststimulation (**d**) or posttransfection (**e**) with synthetic unmodified RNA or synthetic RNAs modified with acp$^3$U (acp$^3$U-8C and acp$^3$U-8D). **f**,**g**, Bubble plots of ingenuity pathway analysis (IPA) analysis of RNA-seq of THP1 macrophages stimulated with acp$^3$U-8C-RNA (**f**) or PNGase F-treated small RNAs (**g**). Activation or repression of pathways is represented by *z*-score (*x* axis and colour) and pathway enrichment by −log-*P* (*y* axis). Dot size is the ratio of the differentially expressed gene (DEG) hits within the total pathway from IPA. **h**, Schematic of the hypothesis in which acp$^3$U exposed on RNA is immunostimulatory, which is attenuated by modifying the carboxylic acid with an amide or GlcNAc. **i**, TNF ELISA of THP1 macrophage supernatants 6 h postaddition or posttransfection with uridine, acp$^3$U, acp$^3$U-modified with an N-acetylglucosamine (acp$^3$U-GlcNAc), acp$^3$U + uridine or acp$^3$U-GlcNAc + uridine. Data are represented as mean ± s.e.m. (**a**–**e**,**i**). Pooled data from three (**a**,**b**,**d**,**e**,**i**) or four (**c**) independent experiments are shown. $^*P < 0.05$; $^{**}P < 0.01$; $^{***}P < 0.001$; $^{****}P < 0.0001$; two-way ANOVA with Tukey's test (**a**,**b**,**d**,**e**,**i**) or one-way ANOVA with Šídák's test (**c**). nt, nucleotide(s).

manner. This effect was not due to increased efferocytosis of apoptotic cells treated with PNGase F as the enzymatic treatment of apoptotic cells did not change efferocytotic rates (Extended Data Fig. 3a). Efferocytosis requires cytoskeleton remodelling within the phagocytes eating the apoptotic cells[32]. When we inhibited efferocytosis of apoptotic cells by pretreating macrophages with actin polymerization inhibitors, cytochalasin D or latrunculin B, we observed a potent reduction in innate immune activation by de-N-glycosylated apoptotic cells as measured by IFNβ production (Fig. 2c). These data indicate that efferocytotic uptake is a prerequisite for de-N-glycosylated apoptotic cells to induce an RNA-driven type I interferon response.

We then asked whether this RNA-dependent inflammatory response was unique to apoptosis induced by doxorubicin or whether this could be recapitulated with ultraviolet-induced apoptosis[33]. We subjected apoptotic HeLa cells generated by means of ultraviolet exposure to PNGase F or PNGase F + RNase treatment and fed them to peritoneal macrophages. We found that ultraviolet-generated apoptotic HeLa cells de-N-glycosylated with PNGase F also induced a robust IFNβ response in an RNA-dependent manner (Fig. 2d). We observed that efferocytosis of de-N-glycosylated apoptotic cells induced IRF3 activation in an RNA-dependent manner in RAW macrophages (Fig. 2e). Similarly, resident peritoneal cells and RAW macrophages also elicited an IFNβ response to de-N-glycosylated apoptotic cells in an RNA-dependent manner (Fig. 2f and Extended Data Fig. 3b). Furthermore, efferocytosis of de-N-glycosylated apoptotic cells induced IL-6 and TNF production in THP1 macrophages and peritoneal macrophages (Fig. 2g and Extended Data Fig. 3c,d). To extend our observations in vivo, we intraperitoneally (i.p.) injected wild-type (WT) mice with apoptotic cells (untreated or PNGase F- or PNGase F + RNase-treated) and then assessed IFNβ levels in the peritoneal lavage 24 hours later. We found IFNβ production only in mice injected with PNGase F-treated apoptotic cells (Fig. 2h). Overall, these data suggest that N-glycosylation of cell surface RNAs facilitates the immunologically 'silent' clearance of apoptotic cells.

## acp$^3$U-modified RNA is immunostimulatory

We recently identified hypermodified acp$^3$U as a site of attachment of N-glycans in sialoglycoRNAs[3]. Mammalian acp$^3$U is synthesized by DTW domain-containing proteins 1 and 2 (DTWD1 and DTWD2) and is best characterized in the D-loop of tRNAs[34]. This discovery offers a genetic approach to prevent the addition of N-glycans on RNA, complementing our pharmacologic strategy of N-glycan removal by PNGase F. Genetic knockout (KO) of DTWD2 led to specific defects in the rPAL profile of sialoglycoRNAs suggesting that DTWD2 is at least in part responsible for sialoglycoRNA biogenesis[3]. We therefore anticipated that DTWD2 deletion would render endogenous small RNAs immunogenic by preventing N-glycan attachment that would otherwise block RNA-dependent innate immune activation. To our surprise, we observed the opposite phenotype: small RNA isolated from DTWD2 KO U2OS cells failed to induce IFNβ production (Fig. 3a and Extended Data Fig. 4a). Similarly, DTWD2 KO apoptotic cells did not induce IFNβ production in macrophages upon efferocytosis, whether untreated or PNGase F-treated (Fig. 3b and Extended Data Fig. 4b). Moreover, DTWD2 KO cell-derived small RNAs and DTWD2 KO apoptotic cells did not induce an RNA-driven innate immune response upon de-N-glycosylation, in THP1 macrophages (Extended Data Fig. 4c,d). Last, DTWD2 KO apoptotic cells untreated or treated with PNGase F failed to induce IFNβ response in vivo upon i.p. injection compared to PNGase F-treated WT apoptotic cells (Fig. 3c).

One possibility that reconciles these results is that acp$^3$U is essential to the immunogenicity of de-N-glycosylated RNA. PNGase F treatment removes entire N-glycan branches to reveal acp$^3$U, the hypermodified base generated by DTWD2 (ref. 3). RNAs harvested from DTWD2 KO cells devoid of acp$^3$U lacked the capacity for IFNβ induction. According to this idea that RNA with exposed acp$^3$U is immunostimulatory, masking acp$^3$U with as little as one N-acetylglucosamine (GlcNAc) could prevent immune activation. To test this, we treated small RNAs with Endo-F2 and Endo-F3 enzymes to yield cleaved glycoRNAs in which acp$^3$U is blocked by a single GlcNAc moiety[3]. Small RNA fractions harvested from WT HeLa cells treated with Endo-F2 + F3 did not induce IFNβ on transfection into RAW or peritoneal macrophages (Extended Data Fig. 4e). Furthermore, unlike PNGase F-treated apoptotic cells, Endo-F2 + F3-treated apoptotic cells did not stimulate IFNβ production during efferocytosis (Extended Data Fig. 4f). Together, these data suggest that exposed acp$^3$U within RNAs can potently induce innate immune responses to endogenous small RNA and apoptotic cells.

Although our data from PNGase F-treated RNA and DTWD2 KO RNA data are consistent, small RNA isolated from cells is complex, made up of many transcripts and other posttranscriptional modifications that could confound our observed phenotype. To confirm a direct role of acp$^3$U, we synthesized an 18-nucleotide long tRNA fragment containing either an unmodified U or acp$^3$U in two sequence contexts (8C and 8D) positioned in the D-loop of a model tRNA (Supplementary Information and Supplementary Table 1). The acp$^3$U-8C and acp$^3$U-8D RNAs have the acp$^3$U within a tRNA D-loop scaffold differing by one nucleobase (GU or AU preceding the acp$^3$U in the 8C and 8D RNAs, respectively). We then used these synthetic RNAs to stimulate THP1 macrophages with or without lipofectamine and found that acp$^3$U containing RNA resulted in higher production of IL-6 and TNF over the unmodified RNA (Fig. 3d,e and Extended Data Fig. 5a,b). To determine the global transcriptional responses induced by acp$^3$U-containing RNAs, we performed bulk RNA sequencing (RNA-seq) of THP1 cells stimulated with acp$^3$U-8C or the unmodified control RNA for 6 hours. Pathway analysis of differentially expressed genes revealed that acp$^3$U-8C induced many pathways related to RNA sensing and innate immune responses such as TLR signalling and IRF pathways. Interferon signalling is the most upregulated pathway in acp$^3$U-8C-RNA-treated cells (Fig. 3f and Extended Data Fig. 5c). We also performed RNA-seq analysis of THP1 cells transfected with untreated or PNGase F-treated small RNAs and found that the immune gene signature induced by PNGase F-treated

RNAs is very similar to that of acp$^3$U-8C RNA with the interferon pathway being the highly expressed one (Fig. 3f,g and Extended Data Fig. 5c–e). Thus, despite the heterogeneity of natural small RNAs compared to the synthetic acp$^3$U-8C RNA, acp$^3$U-8C and PNGase F-treated small RNAs induced a greatly overlapping immune gene signature associated with RNA sensing.

To further examine the immunostimulatory potential of acp$^3$U, we synthesized uridine and acp$^3$U mononucleosides and stimulated or transfected THP1 macrophages and peritoneal macrophages with uridine, acp$^3$U or in combination. When acp$^3$U and uridine are used in combination, we observed an increase in the production of IL-6, TNF and IFNβ suggesting that acp$^3$U with further unmodified uridine bases is more immunostimulatory (Extended Data Fig. 6a–f). Given the selective immune activation upon PNGase F but not Endo-F2 + F3 treatment, we reasoned that the carboxylic acid moiety of acp$^3$U could be critical for its activity. Blocking the carboxylic acid with only a single GlcNAc moiety (acp$^3$U-GlcNAc) or the nitrogen of an amide (acp$^3$U-amide) abrogated the immunogenicity of acp$^3$U when used individually or in combination with extra uridine bases (Fig. 3h,i and Extended Data Fig. 6g,h). Together, these data indicate that acp$^3$U-modified RNA is an innate immune trigger, which supports our model in which N-glycans block the immunostimulatory RNA modification, acp$^3$U, from innate immune sensors.

## TLR3 and TLR7 sense de-N-glycosylated RNAs

To identify the endosomal receptor that senses de-N-glycosylated RNAs, we isolated primary bone-marrow-derived macrophages (BMDMs) from WT, TRIF KO (the adaptor for TLR3) and MyD88 KO (the adaptor for TLR7) mice and stimulated them with small RNA treated with or without PNGase F. We found that PNGase F-treated small RNAs robustly induced an innate immune response compared to untreated RNAs in WT BMDMs, recapitulating our previous results (Fig. 4a). However, IFNβ induction by PNGase F-treated small RNAs was greatly reduced in MyD88 KO and TRIF KO BMDMs, implicating TLR3 and TLR7 as potential receptors for de-N-glycosylated RNAs in mice. Furthermore, to determine whether de-N-glycosylated cell surface RNAs on apoptotic cells activate the MyD88-dependent or TRIF-dependent pathway upon efferocytosis, we induced apoptosis of HeLa cells with doxorubicin and treated the apoptotic cells with PNGase F, RNase or both. These untreated or enzyme-treated apoptotic cells were then fed to WT, MyD88 KO and TRIF KO peritoneal macrophages and the IFNβ response was assessed. IFNβ production induced by PNGase F-treated apoptotic cells was abolished in MyD88 KO and TRIF KO peritoneal macrophages (Fig. 4b). These data show that both MyD88 and TRIF are necessary for innate immune activation by apoptotic cells with de-N-glycosylated cell surface RNAs.

Next, we sought to examine the role of TLR3 and TLR7 in sensing de-N-glycosylated RNAs. We therefore collected peritoneal macrophages and BMDMs from WT, TLR3 KO and TLR7 KO mice and stimulated them with PNGase F-treated or untreated small RNAs (Fig. 4c,d and Extended Data Fig. 7a). Consistent with our previous data, PNGase F-treated small RNAs, compared to untreated RNAs, induced stronger innate immune responses in WT peritoneal macrophages and BMDMs. This effect was also sensitive to RNase treatment as we previously observed. By contrast, de-N-glycosylated small RNA-induced IFNβ production was reduced in both TLR3 KO and TLR7 KO peritoneal macrophages and BMDMs indicating that both receptors are required for optimal sensing of de-N-glycosylated RNA (Fig. 4c,d). We then asked whether TLR3 and TLR7 are also responsible for sensing de-N-glycosylated cell surface RNAs on apoptotic cells during efferocytosis. Like before, we induced apoptosis of HeLa cells with doxorubicin and treated the apoptotic cells. We stimulated WT, TLR3 KO and TLR7 KO peritoneal macrophages with apoptotic cells untreated or treated with PNGase F, RNase or both. Results from WT peritoneal macrophages phenocopied our previous data whereas IFNβ production was ablated in both TLR3 KO and TLR7 KO peritoneal macrophages, supporting our hypothesis that both receptors can detect PNGase F-treated small RNAs (Fig. 4e).

To further examine the role of TLR3 and TLR7 in sensing acp$^3$U-containing RNAs, we stimulated WT, TLR3 KO and TLR7 KO peritoneal macrophages with a synthetic 56-nucleotide long RNA that contains an unmodified uridine or acp$^3$U in the central ssRNA loop and a longer dsRNA region (Supplementary Table 1). We found that stimulation with the acp$^3$U-containing synthetic RNA resulted in the production of IFNβ both by transfection and addition, whereas the unmodified RNA was poorly immunostimulatory (Fig. 4f). More importantly, acp$^3$U-RNA-induced IFNβ response was greatly reduced in TLR3 KO and TLR7 KO macrophages (Fig. 4f). These data showing a dual dependency of synthetic acp$^3$U-RNA on both TLR3 and TLR7 are consistent with the earlier data obtained with de-N-glycosylated cellular RNA. We next tested how the activity of acp$^3$U-RNA compares to well-known TLR3, TLR7 or TLR8 ligands. We stimulated THP1 macrophages individually with de-N-glycosylated small RNAs, unmodified synthetic RNA, acp$^3$U-containing short synthetic RNAs (acp$^3$U-8C and acp$^3$U-8D), poly(I:C) (TLR3), CL097 (TLR7 and TLR8), R837 (TLR7), 2′,3′-cGMP (TLR7), ssRNA40 (TLR7 and TLR8) and TL8 (TLR8) (Extended Data Fig. 7b). We found that de-N-glycosylated small RNAs as well as synthetic acp$^3$U-containing RNAs (acp$^3$U-8C and acp$^3$U-8D) stimulated human THP1 macrophages similarly to other canonical TLR3 and TLR7 or TLR8 ligands. Furthermore, the electroporation of mononucleosides (uridine, acp$^3$U, or acp$^3$U + uridine) as well as the synthetic acp$^3$U-RNAs into the cytosol failed to stimulate an IFNβ response. Consistent with TLR3 and TLR7 sensing of acp$^3$U-RNA, these data indicate that acp$^3$U-RNA are not sensed in the cytosol (Extended Data Fig. 7c). We further corroborated the physiological relevance of these data in vivo by injecting WT, TLR3 KO and TLR7 KO mice i.p. with de-N-glycosylated apoptotic cells and assaying the peritoneal lavage for IFNβ. Consistent with our in vitro findings in peritoneal macrophages, de-N-glycosylated apoptotic cells induced IFNβ production in WT mice but not in TLR3 KO and TLR7 KO mice (Fig. 4g). Altogether, these data show that TLR3 and TLR7 are sensors for de-N-glycosylated RNAs supporting our model that N-glycosylation chemically cages acp$^3$U-containing RNAs preventing them from activating endosomal RNA sensors (Fig. 4h).

Here we describe a mechanism by which glycoRNAs can exist in spaces where highly sensitive RNA sensors exist. We provide evidence that N-glycans serve to chemically cage the hypermodified nucleoside acp$^3$U to prevent self-activation of TLR3 and TLR7. The caging of acp$^3$U in mammalian RNA also promotes homeostatic efferocytosis by blocking the engagement of glycoRNAs present on the surface of apoptotic cells by macrophage TLRs. Methods and experimental strategies capable of assessing the functional role of glycoRNAs are still in their nascent form. Live cell RNase treatment has been used recently to study cell surface RNAs and their roles in processes such as neutrophil recruitment to inflammatory sites[2,15,20,35]. Our data with cell-culture-derived small RNAs, *N*-glycoRNA deficient DTWD2 KO cells, and synthetic acp$^3$U-modified RNAs enabled a direct assessment of the role of N-glycans on RNA in the context of endosomal TLR sensing. Together, our data represent an effort to establish a direct role for N-glycosylation of RNA.

The dual sensing by TLR3 and TLR7 of acp$^3$U-containing RNA species is surprising. Though these RNA-sensing receptors have been classically thought to operate independently, there is some evidence for synergy between these two RNA sensors[36]. One possibility for this phenotype could be that purified and de-N-glycosylated cellular RNA fraction contains dsRNA and ssRNA ligands for TLR3 and TLR7, respectively. Thus, the dual engagement of TLR3 and TLR7 by these RNA ligands provide sufficient signal threshold—which, the engagement of TLR3 or TLR7 alone may fail to induce—to drive IRF-dependent interferon transcription. The 18- and 56-nucleotide long synthetic RNAs each contained ssRNA and dsRNA regions, which may allow the engagement of both TLR3 and TLR7. Even though the longer dsRNAs are stronger

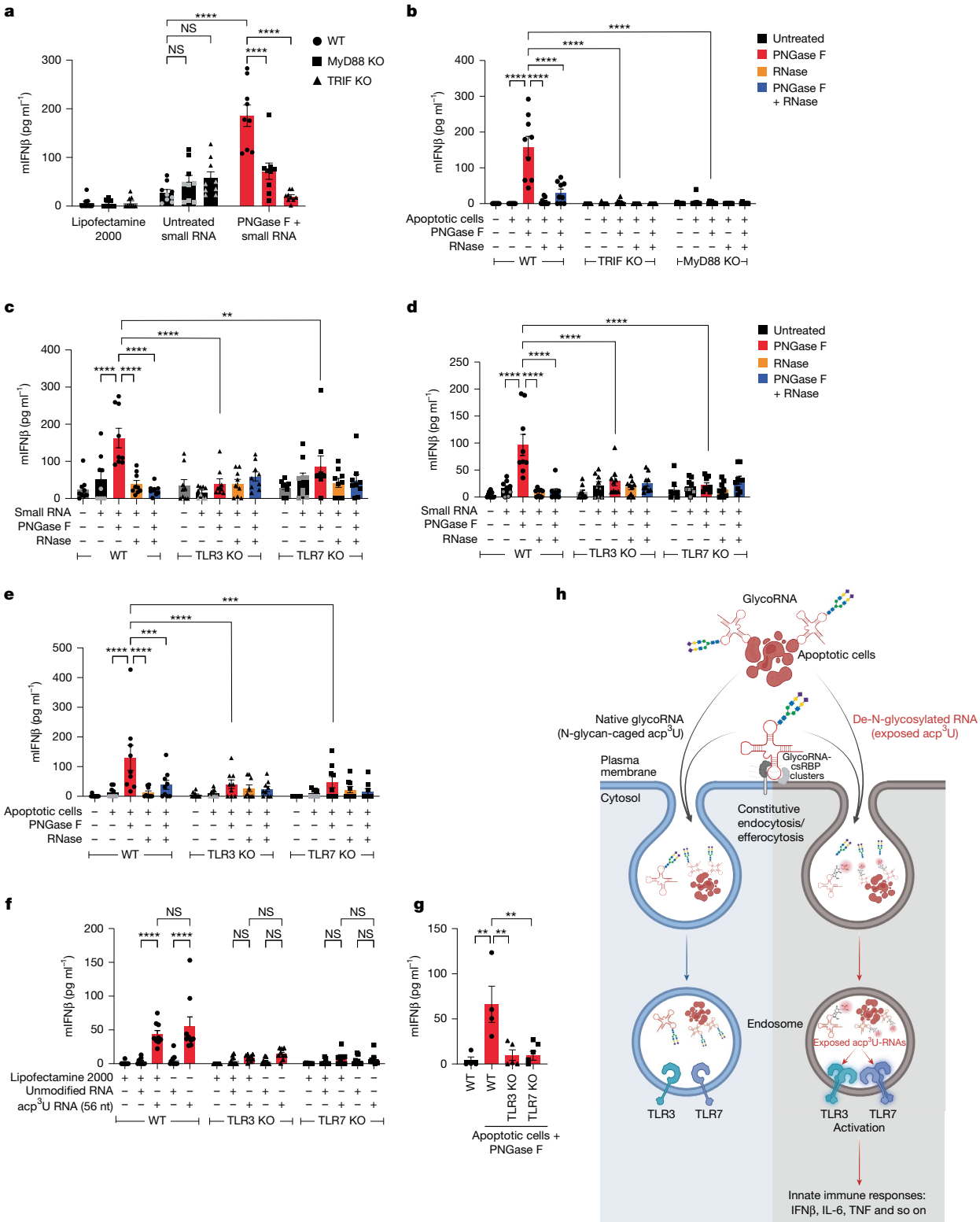


**Fig. 4 | TLR3 and TLR7 sense de-N-glycosylated RNAs. a**, IFNβ ELISA of WT, MyD88 KO and TRIF KO BMDM supernatants 6 h posttransfection with small RNA treated with or without PNGase F. **b**, IFNβ ELISA of WT, MyD88 KO and TRIF KO peritoneal macrophage supernatants 6 h poststimulation with apoptotic HeLa cells treated with or without PNGase F or PNGase F + RNase cocktail at 1:4 macrophage to HeLa cell ratio. **c**, IFNβ ELISA of WT, TLR3 KO and TLR7 KO BMDM supernatants 6 h posttransfection with small RNA treated with or without PNGase F, RNase cocktail, or PNGase F + RNase cocktail. **d**, IFNβ ELISA of WT, TLR3 KO and TLR7 KO peritoneal macrophage supernatants 6 h posttransfection with small RNA treated with or without PNGase F, RNase cocktail or PNGase F + RNase cocktail. **e**, IFNβ ELISA of WT, TLR3 KO and TLR7 KO peritoneal macrophage supernatants 6 h poststimulation with apoptotic HeLa cells treated with or without PNGase F or PNGase F with RNase cocktail at 1:4 macrophage to HeLa cell ratio. **f**, IFNβ ELISA of WT, TLR3 KO, TLR7 KO peritoneal macrophage supernatants 24 h poststimulation with 56-mer synthetic unmodified or acp$^3$U-modified RNAs. **g**, IFNβ ELISA of the peritoneal lavages from WT, TLR3 KO and TLR7 KO mice ($n = 4$) injected with 10 million apoptotic cells treated with or without PNGase F. **h**, Schematic of our model. Data are represented as mean ± s.e.m. (**a**–**g**). Pooled data from three independent experiments are shown (**a**–**g**). $^{**}P < 0.01$; $^{***}P < 0.001$; $^{****}P < 0.0001$. Two-way ANOVA with Tukey's test (**a**–**f**) or one-way ANOVA with Šídák's test (**g**). Schematic in **h** was created in BioRender (https://biorender.com/q27g954).

agonists for TLR3, shorter double-stranded regions have been shown to engage TLR3, albeit weakly[37,38]. Overall, these previously reported observations and the presence of both ssRNA and dsRNA regions in the synthetic RNAs and de-N-glycosylated cellular RNA pool probably explain the dual engagement of TLR7 and TLR3.

In characterizing the RNA component of mouse and human sera, we also identified circulating sialoglycoRNAs. Upon enzymatic de-N-glycosylation, sera-derived glycoRNAs can induce RNA-dependent innate immune activation. This raises the question of whether circulating sialoglycoRNAs could play a causal role in the pathogenesis of diverse autoimmune disorders. Increasing evidence suggests that many autoimmune disorders such as SLE and Aicardi–Goutières syndrome are driven by aberrant sensing of endogenous RNAs[25–28,39]. SLE pathology is associated with the production of anti-dsRNA antibodies[40,41] and auto-antibodies to SSA/Ro and SSB/La proteins that form complexes with Y RNA[42] as well as to Sm proteins that associate with snRNA (U RNAs)[43]. As the major form of glycoRNAs consist of Y RNA[2], it is interesting to speculate whether anti-RNA antibodies are recognizing circulating sialoglycoRNAs or their de-N-glycosylated byproducts such as free or exposed-acp$^3$U and whether such anti-sialoglycoRNA or anti-acp$^3$U antibodies have a role in SLE. Our rPAL data from a small cohort of serum samples from patients with SLE revealed a highly heterogenous pattern with different levels and molecular weights of the observed sialoglycoRNAs. Future studies involving larger cohorts of patients with SLE are warranted to examine whether there is any correlation between the sialoglycoRNA and free or exposed-acp$^3$U levels in the circulation and SLE manifestations and establish a clinical link between RNA with uncaged acp$^3$U and SLE. We also observed that PNGase F-treated small RNA could activate both human pDCs and macrophages, two cell types that have been associated with the pathogenesis of SLE[44–47], suggesting that these small RNAs could contribute to SLE and potentially other autoimmune diseases.

Finally, although we describe the presence of acp$^3$U on RNA as an immunostimulatory modification, there are other putative linkers between N-glycans and RNA such as yW-72 and yW-86 that have not yet been fully characterized and remain under active investigation[3]. Examining the expression patterns of the enzymes making these modifications, their deposition in RNA and the biodistribution of these RNAs and their caged forms in autoimmune disease could provide new insights into the development of autoimmunity and potential therapeutic targets.

## Online content

Any methods, additional references, Nature Portfolio reporting summaries, source data, extended data, supplementary information, acknowledgements, peer review information; details of author contributions and competing interests; and statements of data and code availability are available at https://doi.org/10.1038/s41586-025-09310-6.


1. Varki, A. et al. *Essentials of Glycobiology* 3rd edn (Cold Spring Harbor Laboratory Press, 2015).
2. Flynn, R. A. et al. Small RNAs are modified with N-glycans and displayed on the surface of living cells. *Cell* **184**, 3109–3124 (2021).
3. Xie, Y. et al. The modified RNA base acp3U is an attachment site for N-glycans in glycoRNA. *Cell* **187**, 5228–5237.e12 (2024).
4. Alexopoulou, L., Holt, A. C., Medzhitov, R. & Flavell, R. A. Recognition of double-stranded RNA and activation of NF-kappaB by Toll-like receptor 3. *Nature* **413**, 732–738 (2001).
5. Diebold, S. S., Kaisho, T., Hemmi, H., Akira, S. & Reis e Sousa, C. Innate antiviral responses by means of TLR7-mediated recognition of single-stranded RNA. *Science* **303**, 1529–1531 (2004).
6. Heil, F. et al. Species-specific recognition of single-stranded RNA via Toll-like receptor 7 and 8. *Science* **303**, 1526–1529 (2004).
7. Greulich, W. et al. TLR8 is a sensor of RNase T2 degradation products. *Cell* **179**, 1264–1275 (2019).
8. Asami, J. & Shimizu, T. Structural and functional understanding of the Toll-like receptors. *Protein Sci.* **30**, 761–772 (2021).
9. Yoneyama, M. et al. The RNA helicase RIG-I has an essential function in double-stranded RNA-induced innate antiviral responses. *Nat. Immunol.* **5**, 730–737 (2004).
10. Kato, H. et al. Length-dependent recognition of double-stranded ribonucleic acids by retinoic acid-inducible gene-I and melanoma differentiation-associated gene 5. *J. Exp. Med.* **205**, 1601–1610 (2008).
11. Sato, M. et al. Positive feedback regulation of type I IFN genes by the IFN-inducible transcription factor IRF-7. *FEBS Lett.* **441**, 106–110 (1998).
12. Juang, Y. T. et al. Primary activation of interferon A and interferon B gene transcription by interferon regulatory factor 3. *Proc. Natl Acad. Sci. USA* **95**, 9837–9842 (1998).
13. Huang, Y. et al. TLR7 promotes skin inflammation via activating NFκB-mTORC1 axis in rosacea. *PeerJ* **11**, e15976 (2023).
14. Nainytė, M., Amatov, T. & Carell, T. Synthesis of an acp. *Chem. Commun.* **55**, 12216–12218 (2019).
15. Ma, Y. et al. Spatial imaging of glycoRNA in single cells with ARPLA. *Nat. Biotechnol.* **42**, 608–616 (2023).
16. Ren, Z. et al. Enzyme-mediated proximity labeling identifies small RNAs in the endoplasmic reticulum lumen. *Biochemistry* **62**, 1844–1848 (2023).
17. Arandjelovic, S. & Ravichandran, K. S. Phagocytosis of apoptotic cells in homeostasis. *Nat. Immunol.* **16**, 907–917 (2015).
18. Kawano, M. & Nagata, S. Efferocytosis and autoimmune disease. *Int. Immunol.* **30**, 551–558 (2018).
19. Xie, Y. et al. Development and application of GlycanDIA workflow for glycomic analysis. Preprint at *bioRxiv* https://doi.org/10.1101/2024.03.12.584702 (2024).
20. Perr, J. et al. RNA-binding proteins and glycoRNAs form domains on the cell surface for cell-penetrating peptide entry. *Cell* https://doi.org/10.1016/j.cell.2025.01.040 (2025).
21. Kawai, T., Ikegawa, M., Ori, D. & Akira, S. Decoding Toll-like receptors: recent insights and perspectives in innate immunity. *Immunity* **57**, 649–673 (2024).
22. Fisch, D. et al. Molecular definition of the endogenous Toll-like receptor signalling pathways. *Nature* **631**, 635–644 (2024).
23. Godoy, P. M. et al. Large differences in small RNA composition between human biofluids. *Cell Rep.* **25**, 1346–1358 (2018).
24. Srinivasan, S. et al. Small RNA sequencing across diverse biofluids identifies optimal methods for exRNA isolation. *Cell* **177**, 446–462 (2019).
25. Brown, G. J. et al. TLR7 gain-of-function genetic variation causes human lupus. *Nature* **605**, 349–356 (2022).
26. Satterthwaite, A. B. TLR7 signaling in lupus B cells: new insights into synergizing factors and downstream signals. *Curr. Rheumatol. Rep.* **23**, 80 (2021).
27. Dorrity, T. J. et al. Long 3′UTRs predispose neurons to inflammation by promoting immunostimulatory double-stranded RNA formation. *Sci. Immunol.* **8**, eadg2979 (2023).
28. Maharana, S. et al. SAMHD1 controls innate immunity by regulating condensation of immunogenic self RNA. *Mol. Cell* **82**, 3712–3728 (2022).
29. Davis, P., Cunnington, P. & Hughes, G. Double-stranded RNA antibodies in systemic lupus erythematosus. *Ann. Rheum. Disease.* **34**, 239 (1975).
30. Boada-Romero, E., Martinez, J., Heckmann, B. L. & Green, D. R. The clearance of dead cells by efferocytosis. *Nat. Rev. Mol. Cell Biol.* **21**, 398–414 (2020).
31. Lee, S. J. et al. Transactivation of bad by vorinostat-induced acetylated p53 enhances doxorubicin-induced cytotoxicity in cervical cancer cells. *Exp. Mol. Med.* **46**, e76 (2014).
32. Elliott, M. R. & Ravichandran, K. S. The dynamics of apoptotic cell clearance. *Dev. Cell* **38**, 147–160 (2016).
33. Piva, T. J., Davern, C. M., Hall, P. M., Winterford, C. M. & Ellem, K. A. O. Increased activity of cell surface peptidases in HeLa cells undergoing UV-induced apoptosis is not mediated by caspase 3. *Int. J. Mol. Sci.* **13**, 2650–2675 (2012).
34. Takakura, M., Ishiguro, K., Akichika, S., Miyauchi, K. & Suzuki, T. Biogenesis and functions of aminocarboxypropyluridine in tRNA. *Nat. Commun.* **10**, 5542 (2019).
35. Zhang, N. et al. Cell surface RNAs control neutrophil recruitment. *Cell* **187**, 846–860 (2024).
36. Liu, B. et al. Innate immune memory and homeostasis may be conferred through crosstalk between the TLR3 and TLR7 pathways. *Sci. Signal.* **9**, ra70 (2016).
37. Sakaniwa, K. et al. TLR3 forms a laterally aligned multimeric complex along double-stranded RNA for efficient signal transduction. *Nat. Commun.* **14**, 164 (2023).
38. Leonard, J. N. et al. The TLR3 signaling complex forms by cooperative receptor dimerization. *Proc. Natl Acad. Sci. USA* **105**, 258–263 (2008).
39. Barrat, F. J., Elkon, K. B. & Fitzgerald, K. A. Importance of nucleic acid recognition in inflammation and autoimmunity. *Annu. Rev. Med.* **67**, 323–336 (2016).
40. Koffler, D., Agnello, V. & Kimkel, H. G. Polynucleotide immune complexes in serum and glomeruli of patients with systemic lupus erythematosus. *Am. J. Pathol.* **74**, 109–124 (1974).
41. Jenks, S. A. et al. B cell subset composition segments clinically and serologically distinct groups in chronic cutaneous lupus erythematosus. *Ann. Rheum. Dis.* **80**, 1190–1200 (2021).
42. Franceschini, F. & Cavazzana, I. Anti-Ro/SSA and La/SSB antibodies. *Autoimmunity* **38**, 55–63 (2005).
43. Migliorini, P., Baldini, C., Rocchi, V. & Bombardieri, S. Anti-Sm and anti-RNP antibodies. *Autoimmunity* **38**, 47–54 (2005).
44. Ah Kioon, M. D. et al. Modulation of plasmacytoid dendritic cells response in inflammation and autoimmunity. *Immunol. Rev.* **323**, 241–256 (2024)
45. Barrat, F. J. & Su, L. A pathogenic role of plasmacytoid dendritic cells in autoimmunity and chronic viral infection. *J. Exp. Med.* **216**, 1974–1985 (2019).
46. Reizis, B. Plasmacytoid dendritic cells: development, regulation, and function. *Immunity* **50**, 37–50 (2019).
47. Kuriakose, J. et al. Patrolling monocytes promote the pathogenesis of early lupus-like glomerulonephritis. *J. Clin. Invest.* **129**, 2251–2265 (2019).

# Methods

### Mice

WT C57BL/6J, TLR3 KO (strain B6;129S1-Tlr3tm1Flv/J), TLR7 KO (strain B6.129S1-Tlr7tm1Flv/J), MyD88 KO (strain B6.129P2(SJL)-Myd88/J) and TRIF KO (strain C57BL/6J-Ticam1/J) from the Jackson Laboratory were bred and maintained in specific pathogen-free conditions in the animal facility of UConn Health. All mice were housed at an ambient temperature of roughly 22 °C, a humidity of 40–60% and a light/dark cycle of 12/12 h. Sex- and age-matched mice were used. All experiments were carried out in accordance with the guidelines set forth by the UConn Health Institutional Animal Care and Use Committee.

### Cells

HeLa cells (American Type Culture Collection (ATCC), CCL-2), U2OS (ATCC, HTB-96), U2OS DTWD2 KO (clones 1 and 2 from ref. 3) and RAW 264.7 cells (ATCC, TIB-71) were maintained in Dulbecco's modified Eagle media (DMEM, Gibco) supplemented with 10% heat-inactivated fetal bovine serum (FBS) (SeraPrime) and 1% penicillin–streptomycin (Invitrogen). HeLa and U2OS cells were passaged with TrypLE (Gibco). THP1 (ATCC, TIB-202) cells were maintained in RPMI 1640 (Gibco) containing 10% FBS and 1% penicillin–streptomycin. Cell lines were authenticated by the sources and no further validation was done. THP1 monocytes were seeded and differentiated into macrophages with 100 ng $ml^{-1}$ phorbol 12-myristate-13-acetate (catalogue no. 10008014; Cayman Chemical) overnight. Peritoneal macrophages were obtained by peritoneal lavage of 4 days of thioglycollate-injected (Remel, catalogue no. R07178) mice, euthanized with $CO_2$. Resident peritoneal cells were similarly obtained from naïve mice. Peritoneal macrophages and resident peritoneal cells were cultured in DMEM with 10% FBS and 1% penicillin–streptomycin. To generate primary BMDMs, bone marrow cells from femurs and tibiae of mice were cultured in 10% FBS DMEM containing 20% L929 conditioned supernatant, with media replacement on days 3 and 6.

### RNA isolation and fractionation

HeLa cells were seeded into 15-cm cell culture plates and grown until roughly 70% confluency. Media was removed and 2 ml of RNAzol RT (Molecular Research Center) was used to lyse and isolate small or large RNA fractions according to the manufacturers protocol. Briefly, water was added to precipitate DNA, proteins and lipids followed by precipitation of large RNAs with 100% ethanol. Small RNAs were isolated from the supernatant postlarge RNA precipitation by precipitating with 100% isopropanol. Large and small RNAs were then cleaned using a Zymo Clean and Concentrator Kit (Zymo Research) and then eluted in UltraPure DNase/RNase free water (Invitrogen). To harvest small RNAs from WT mice and commercial human sera samples (Pel-Freez and Innovative Research), we added 1 ml of RNAzol RT to 400 µl of sera and isolated the small RNA fraction as described above.

### RNA stimulation of cells

Large RNAs (300 ng), small RNAs (30 or 300 ng) or poly(I:C) (300 ng) (catalogue no. tlrl-pic-5; InvivoGen) were treated in Opti-Mem (Gibco) with or without 2 µl (2 µg; for three wells of 100,000 cells/well) of PNGase F Prime (Bulldog Bio), 2 µl of an RNase cocktail (ThermoFisher) with 1 µl of RNase III (New England Biolabs) for 2 h at 37 °C. After digestion, each condition was transfected using Lipofectamine 2000 (ThermoFisher) into 100,000 indicated cells for 6 h or column cleaned using Zymo RNA Clean and Concentrator kit (R1013, Zymo Research) and then transfected into cells. Furthermore, all synthetic ligands generated in this study were added (directly to cell culture supernatant) or transfected into cells using Lipofectamine 2000 (ThermoFisher) as previously described. The supernatant was then assayed for various cytokines by enzyme-linked immunosorbent assay (ELISA).

### Electroporation

Electroporation of synthetic unmodified or $acp^3U$-containing mononucleosides and 18-mer RNAs were performed using the ThermoFisher Neon transfection system according to the manufacturer's protocol. Then $2 \times 10^5$ RAW 264.7 cells were mixed with each ligand and then the electroporation was done using the following settings: 1,680 V, 20 ms and 1 pulse. Cells were then seeded in DMEM containing 10% FBS (no antibiotic) for 24 h. Supernatant was then assayed for IFNβ by ELISA.

### rPAL labelling and northern blotting of glycoRNAs

rPAL and northern blotting were performed as previously described[3]. Briefly, lyophilized RNA (3 µg of HeLa total RNA or 1 µg of sera RNA) was blocked in a 28 µl of reaction containing 570 µM mPEG3-Ald (BroadPharm, catalogue no. BP-22802), 500 mM $MgSO_4$ and 450 mM $NH_4OAc$ pH 5.0 for 45 min at 35 °C. Then 1 µl of 30 mM aldehyde reactive probe (Cayman Chemicals, ARP/aminooxy biotin, catalogue no. 10009350) and 2 µl of 7.5 mM $NaIO_4$ were added, quickly vortexed and incubated for 10 min at room temperature in the dark. The reaction was quenched with the addition of 3 µl of 22 mM sodium sulfite for 5 min at room temperature in the dark, and the ligation reaction was allowed to proceed for 90 min at 35 °C in the dark. Labelled RNA was cleaned using a Zymo-I column (Zymo Research, catalogue no. C1003) and RNA was eluted from the column with 2× 25 µl of water and subsequently lyophilized. Lyophilized RNA was resuspended in 12 µl of water and 12 µl of Gel Loading Buffer II (95% formamide, 18 mM EDTA, 0.025% SDS) with 5× SYBR Gold (ThermoFisher Scientific, catalogue no. S11494), denatured for 10 min at 55 °C and snap chilled on ice for 2 min before loading on a 1% agarose, 0.75% formaldehyde, 1.5× MOPS (Lonza, catalogue no. 50876) denaturing gel. The gel was run for 34 min at 115 V in 1× MOPS buffer, visualized on an ultraviolet imager and transferred to a nitrocellulose membrane in 3 M NaCl pH 1.0 for 90 min. Membranes were blocked with Intercept Protein-Free Blocking Buffer (LiCor Biosciences, catalogue no. 927-80001) for 30 min at room temperature and stained with 1:5,000 Streptavidin IR800 (LiCor Biosciences, catalogue no. 926-32230) diluted in blocking buffer for 30 min at room temperature, followed by washes with 1× phosphate-buffered saline (PBS) + 0.1% Tween-20 (Sigma, catalogue no. P1379) and 1× PBS. Membranes were imaged on a LiCor Odyssey CLx scanner (LiCor Biosciences).

### Immunoblotting

After stimulation, cell lysates were prepared using RIPA buffer containing protease inhibitor cocktail (catalogue no. 1861279; ThermoFisher) and phosphatase inhibitor (catalogue no. 78420; ThermoFisher), run on 10 or 12.5% polyacrylamide gel and transferred to nitrocellulose membranes. Membranes were then probed with the following antibodies. phospho-IRF3 (1:1,000 dilution, 4D4G, 4947, Cell Signaling Technology), total IRF3 (1:1,000 dilution, 4302, D83B9, Cell Signaling Technology), total TBK1 (1:1,000 dilution, 51872, E9H5S, Cell Signaling Technology), phospho-TBK1 (1:1,000 dilution, 5483, D52C2, Cell Signaling Technology) and α-Tubulin (1:1,000 dilution, 3873, DM1A, Cell Signaling Technology), phospho-p38 (1:1,000 dilution, 4511 (Thr180/Tyr182, D3F9), Cell Signaling Technology), total p38 (1:1,000 dilution, 8690 (D13E1), Cell Signaling Technology), phospho-p65 (1:1,000 dilution, 3031 (Ser536), Cell Signaling Technology), total p65 (1:1,000 dilution, 6956 (L8F6), Cell Signaling Technology), phospho-JNK (1:1,000 dilution, 9251 (Thr183/Tyr185), Cell Signaling Technology), total JNK (1:1,000 dilution, 9252, Cell Signaling Technology), phospho-ERK1/2 (1:1,000 dilution, 9106 (Thr202/Tyr204), Cell Signaling Technology), total ERK1/2 (1:1,000 dilution, 9102, Cell Signaling Technology) and β-Actin (1:1,000, 3700 (8H10D10), Cell Signaling Technology). Secondary antibodies used were HRP-conjugated anti-rabbit (1:5,000 dilution, 711035152, Jackson ImmunoResearch), HRP-conjugated

anti-mouse (1:5,000 dilution, 115035166, Jackson ImmunoResearch) and HRP-conjugated anti-goat (1:5,000 dilution, 805035180, Jackson ImmunoResearch) diluted in 5% milk in Tris-buffered saline with Tween. Blots were then imaged using an Azure 800 imager.

### Co-immunoprecipitation

Co-immunoprecipitation of the myddosome assembly was performed as previously described[22]. Briefly primary BMDM cells were seeded into a six-well plate and stimulated with Pam3CSK4 (1 μg $ml^{-1}$) as a positive control and small RNAs treated with or without PNGase F (Bulldog Bio) or in combination with RNase cocktail (ThermoFisher and New England Biolabs). After 3 h, cells were lysed with ice cold 1% NP-40 lysis buffer containing protease inhibitor cocktail (ThermoFisher) and phosphatase inhibitor (ThermoFisher) for 15 min at 4 °C, centrifuged to remove cellular debris and then incubated overnight with anti-MyD88 antibody (AF3109, R&D Systems) and Protein G magnetic beads (Pierce Protein G Magnetic Beads, catalogue no. 88847, Thermo Scientific). Next, beads were washed five times with ice cold NP-40 lysis buffer. Samples were then run on a 10% SDS–PAGE gel as previously described and blotted for IRAK2 (1:1,000 dilution, 4367T, Cell Signaling Technology), TIRAP (1:1,000 dilution, 13077T, Cell Signaling Technology), MyD88 (1:1,000 dilution, AF3109, R&D systems) and β-Actin (1:1,000, 3700 (8H10D10), Cell Signaling Technology). Blots were then imaged using an Azure 800 imager.

### Preparation and culture of primary human macrophages and pDCs

Enriched leukocytes were obtained from the New York Blood Center after informed consent of the donor and used under a protocol approved by the Institutional Review Board of the Hospital for Special Surgery and the Institutional Biosafety Committee of Weill Cornell Medical College. Peripheral blood mononuclear cells were prepared using Ficoll–Paque density gradient (GE Healthcare) as previously described[48]. pDCs and monocytes were isolated by positive selection using BDCA4-conjugated microbeads 2 and CD14-conjugated microbeads 3 (Miltenyi), respectively. Macrophages were differentiated from monocytes by culturing with 20 ng $ml^{-1}$ macrophage colony-stimulating factor for 5 days. For functional assay, freshly isolated pDCs were resuspended at 0.3–0.4 × $10^5$ cells per 100 μl of RPMI 1640 medium (Gibco) and cultured for 24 h and then transfected with 100 ng of small RNA that were either untreated or treated with PNGase F (Bulldog Bio) using Lipofectamine 3000 (Invitrogen). After differentiation of macrophages, the cells were cultured at 1 × $10^5$ cells per 100 μl RPMI 1640 medium for 24 h and then transfected with 100 ng of small RNA that were either untreated or treated with PNGase F (Bulldog Bio) using Lipofectamine 3000 (Invitrogen). After 24 h, supernatant was collected for cytokine analysis by ELISA according to the manufacturer's protocol (MabTech).

### In vitro and in vivo efferocytosis assays

To induce apoptosis, we subjected HeLa cells to 4 μM of doxorubicin (catalogue no. 15007; Caymen Chemical) or 0.24 J $cm^{-2}$ of ultraviolet light and incubated overnight. Dimethylsulfoxide (DMSO)-treated live HeLa cells were used as a control. Next, cells were collected, centrifuged at 4,000*g* for 10 min and resuspended in serum-free media. Apoptotic cells were treated with or without PNGase F Prime (catalogue no. NZPULT10LY; Bulldog Bio) and RNase cocktail (catalogue no. AM2286; ThermoFisher) combined with RNase III (catalogue no. M0245S; New England BioLabs) for 2 h at 37 °C. Control and enzyme-treated apoptotic cells were fed to peritoneal macrophages, RAW 264.7 cells and human THP1 macrophages for 6 or 24 h. Supernatant of efferocytotic macrophages were then assayed for cytokines by ELISA. In certain experiments, peritoneal macrophages were pretreated with actin polymerization inhibitors cytochalasin D (catalogue no. BML-T109; Enzo Life Sciences) and latrunculin B (catalogue no. BML-T110; Enzo Life Sciences) to inhibit efferocytosis and then stimulated with PNGase F-treated apoptotic cells. Furthermore, WT mice were injected i.p. with 10 million untreated, PNGase F or RNase-treated apoptotic cells, and after 24 h peritoneal lavages were collected and concentrated using Microsep Advanced centrifugal concentrator with a 3-kDa filter (Pall Corporation) for cytokine analysis by ELISA.

### High dose PNGase F treatment of RAW cells

RAW 264.7 cells (100,000/well) were seeded overnight to rest. Next, the media was replaced with fresh media containing either 2, 6 or 10 μg of PNGase F (Bulldog Bio) or identical doses containing 1 μl of RNase cocktail (ThermoFisher). Treated cells were incubated overnight and supernatant was collected for IFNβ ELISA.

### Flow cytometry of efferocytotic peritoneal macrophages

Live and apoptotic HeLa cells were treated with PNGase F or PNGase F with an RNase cocktail for 2 h and stained with CellBright Red membrane dye (Biotium) according to the manufacturer's protocol. CellBright Red-labelled live and apoptotic HeLa cells were then fed to peritoneal macrophages at a ratio of 1:4 (macrophages to HeLa cells) for 2 h. Macrophages were then washed with fluorescence-activated cell sorting buffer (PBS containing 2.5% FBS and 2 mM EDTA) and stained with APC-conjugated anti-CD11b antibody (catalogue no. 101211; Biolegend). Flow cytometric analysis was performed on a FACSymphony A5 (BD Biosciences) and data were then processed by using FlowJo (BD Biosciences, v.10.10).

### Synthesis and purification of oligonucleotides

Phosphoramidites of canonical ribonucleosides (Bz-A-CE, ibu-G-CE, Ac-C-CE and U-CE) were purchased from Sigma-Aldrich. Oligonucleotides were synthesized on a 1-μmol scale using RNA SynBase CPG 1000/110 and High Load Glen UnySupport as solid supports using an RNA automated synthesizer (Applied Biosystems 394 DNA/RNA Synthesizer) with a standard phosphoramidite chemistry. Oligonucleotides were synthesized in 5′-trityl-OFF mode using dichloroacetic acid (DCA) as a deblocking agent in $CH_2Cl_2$, Activator 42 as activator in MeCN, $Ac_2O$ as capping reagent in pyridine/THF and $I_2$ as oxidizer in pyridine/$H_2O$.

### Cleavage from beads and precipitation of the oligonucleotide

The solid support beads were suspended in a 1:1 aqueous solution mixture (0.6 ml) of 30% $NH_4OH$ and 40% $MeNH_2$. The suspension was heated at 65 °C (8 min for SynBase CPG 1000/110 and 60 min for High Load Glen UnySupport). Subsequently, the supernatant was collected, and the beads were washed with water (2 × 0.3 ml). The combined aqueous solutions were concentrated under reduced pressure using a SpeedVac concentrator. After that, the TBS-protecting group of the 2′-OH was cleaved by incubation of the oligonucleotide in DMSO (100 μl) and HF•$NEt_3$ (100 μl) at 65 °C for 1.5 h, and the oligonucleotide was precipitated by adding 3 M NaOAc in water (25 μl) and *n*-butanol (1 ml). The mixture was kept at −80 °C for 2 h and centrifuged at 4 °C for 1 h. The supernatant was removed and the white precipitate was lyophilized.

### Purification of the oligonucleotides by HPLC and desalting

The crude mixture was purified by semipreparative high-performance liquid chromatography (HPLC) (1260 Infinity II Manual Preparative Liquid Chromatography System from Agilent equipped with a G7114A detector) using a reverse-phase (RP) VP 250/10 Nucleodur 100-5 C18ec column from Macherey-Nagel (buffer A 0.1 M AcOH:$Et_3N$, pH 7 in $H_2O$ and buffer B 0.1 M AcOH:$Et_3N$, pH 7 in 20:80 $H_2O$:MeCN; gradient 0–25% of B in 45 min; flow rate 5 ml $min^{-1}$). The purified oligonucleotide was analysed by RP-HPLC (1260 Infinity II Liquid Chromatography System from Agilent equipped with a G7165A detector) using an EC 250/4 Nucleodur 100-3 C18ec from Macherey-Nagel (gradient 0–30% of B in

45 min; flow rate 1 ml $min^{-1}$). Finally, the purified oligonucleotide was desalted using a C18 RP-cartridge from Waters.

### Determination of concentration and mass of oligonucleotide

The absorbance of the synthesized oligonucleotide in $H_2O$ solution was measured using an IMPLEN NanoPhotometer N60/N50 at 260 nm. The extinction coefficient of the oligonucleotide was calculated using the OligoAnalyzer v.3.0 from Integrated DNA Technologies. For oligonucleotides incorporating non-canonical bases, the extinction coefficients were assumed to be identical to those containing only canonical counterparts. The synthesized oligonucleotide (2–3 µl) was desalted on a 0.025-µm VSWP filter (Millipore), cocrystallized in a 3-hydroxypicolinic acid matrix (1 µl) and analysed by matrix-assisted laser desorption/ionization–time-of-flight mass spectrometry (negative mode).

### ELISA

Mouse IFNβ ELISA was performed as described previously[49] using an anti-IFNβ monoclonal antibody (sc-57201, Santa Cruz Biotechnology) as a capture antibody and a rabbit polyclonal anti-mouse IFNβ antibody (32400-1, PBL Assay Science) as a detection antibody. Human TNF (88-7346-88, Invitrogen), human IL-6 (88-7066-88, Invitrogen), mouse IL-6 (88-7064-88, Invitrogen), mouse TNF (88-7324-88, Invitrogen) and human IFNα (3425-1H-6, MabTech) ELISAs were performed according to the manufacturer's protocol.

### Human SLE samples

Patients were enrolled in a research study for suspected neuroinflammatory disease (University of California, San Francisco, Institutional Review Board no. 13-12236). Serum samples were frozen and stored at −80 °C before aliquoting as undiluted serum or diluted 1:1 in antibody sample buffer (final concentration: 20% glycerol, 20 mM HEPES and 0.02% sodium azide in PBS).

### RNA-seq analysis

Total RNA was extracted from THP1 macrophages stimulated with unmodified RNA, $acp^3U$-8C-RNA, untreated small RNA or PNGase F-treated small RNAs for 6 h as described above using the Zymo Direct-zol (catalogue no. R2052; Zymo). After quality checking, total RNA samples were subjected to Illumina Stranded Ligation messenger RNA library preparation followed by Illumina NovaSeq S4 v.1.5 for 200 cycles with 40 million total paired-end reads per sample at the Center for Genome Innovation, Institute for Systems Genomics, University of Connecticut. The raw data were demultiplexed using Illumina's bcl2fastq v.2.20. Reads in FASTQ files were aligned using HISAT2 v.2.2.1 (ref. 50) on the GRCh38 index, with SAMtools v.1.9 (ref. 51) for BAM conversion. Fragments per kilobase of transcript per million fragments mapped was calculated from aligned reads using StringTie v.2.1.3 with Ballgown[52,53].

Data analyses were conducted with R v.4.4.0. Gene expressions were filtered by a minimum detection in at least one sample, yielding 32,389 unique gene IDs. The filtered fragments per kilobase of transcript per million fragments mapped matrix was $\log_2$ transformed and normalized by quantiles using NormalizeBetweenArrays function from limma v.3.60.2 R package[54]. For differential gene expression, the limma-trend method[52,53] was used: genes with an absolute $\log_2$ fold change greater than 1.5 were considered differentially expressed. For gene-expression visualization, expression *z*-score was calculated by mean (gene expression)/standard deviation (gene expression). Gene ontology was performed on differentially expressed genes using the QIAGEN IPA (Qiagen Inc., https://digitalinsights.qiagen.com/IPA)[55]. RNA-seq datasets generated in this study are available from the Gene Expression Omnibus (accession number GSE291767).

### Statistical analysis

Data were analysed for statistical significance by unpaired two-tailed *t*-test or one-way or two-way ANOVA as indicated in the figure legends. No blinding and randomization were performed in this study. Statistical methods were not used to predetermine sample size. Data were plotted and analysed using Prism Graphpad software v.10.1.2. Figures were generated with Adobe Illustrator v.28.5. RNA-seq data analyses were conducted with R v.4.4.0.

### Reporting summary

Further information on research design is available in the Nature Portfolio Reporting Summary linked to this article.

## Data availability

RNA-seq data have been deposited and are accessible at Gene Expression Omnibus number GSE291767. Source data are provided with this paper.


48. Du, Y. et al. Chemokines form nanoparticles with DNA and can superinduce TLR-driven immune inflammation. *J. Exp. Med.* **219**, e20212142 (2022).
49. Roberts, Z. J. et al. The chemotherapeutic agent DMXAA potently and specifically activates the TBK1-IRF-3 signaling axis. *J. Exp. Med.* **204**, 1559–1569 (2007).
50. Kim, D., Paggi, J. M., Park, C., Bennett, C. & Salzberg, S. L. Graph-based genome alignment and genotyping with HISAT2 and HISAT-genotype. *Nat. Biotechnol.* **37**, 907–915 (2019)
51. Danecek, P. et al. Twelve years of SAMtools and BCFtools. *Gigascience* **10**, giab008 (2021).
52. Pertea, M. et al. StringTie enables improved reconstruction of a transcriptome from RNA-seq reads. *Nat. Biotechnol.* **33**, 290–295 (2015).
53. Frazee, A. C. et al. Ballgown bridges the gap between transcriptome assembly and expression analysis. *Nat. Biotechnol.* **33**, 243–246 (2015).
54. Ritchie, M. E. et al. limma powers differential expression analyses for RNA-sequencing and microarray studies. *Nucleic Acids Res.* **43**, e47 (2015).
55. Krämer, A., Green, J., Pollard, J. & Tugendreich, S. Causal analysis approaches in ingenuity pathway analysis. *Bioinformatics* **30**, 523–530 (2014).



**Acknowledgements** We thank the members of the Rathinam and Flynn laboratories for their constructive feedback. We also thank C. Bertozzi and N. Till for the synthesis of stereoisomerically pure $acp^3U$, P. Sharp for helpful discussions, V. Hornung and M. Berouti for technical help and P. Hristov for chemical drawings. This work was supported by grants from Burroughs Wellcome Fund Career Award for Medical Scientists (R.A.F.), The Rita Allen Foundation (R.A.F.), The Sontag Foundation (R.A.F.), The Scleroderma Research Foundation (R.A.F. and F.J.B.) and National Institute of General Medical Sciences, National Institute of Diabetes and Digestive and Kidney Diseases, and the National Institute of Allergy and Infectious Diseases of the National Institutes of Health under grant award numbers F31AI178967 (V.R.G.), R35GM151157 (R.A.F.), R01AI119015 (V.A.R.), R01AI148491 (V.A.R.), R01AI132850 (S.K.V.), R01DK121805 (B.Z.) and R01HL172239 (B.Z.), the Deutsche Forschungsgemeinschaft (DFG) CA275/11-3 (ID 326039064), CRC1309 (ID 325871075, A4), CRC1361 (ID 393547839, P2) and TRR237 (ID 369799452, A27) and the European Research Council (ERC) under grant no. 741912 (EPiR) (T.C.).


**Author contributions** V.R.G., R.A.F. and V.A.R. conceived the project, designed experimental strategies, analysed the data, generated the figures and wrote the manuscript. V.R.G. and J.P. performed experiments. J.P. and C.G.L. performed rPAL analysis. P.C. generated DTWD2 KO cells. I.M. and T.C. designed and synthesized mononucleosides as well as unmodified and modified synthetic RNA. J.V.P. and M.R.W. collected and processed the human SLE samples. M.D.A.K. and F.J.B. isolated and performed human pDC and primary macrophage assays. A.J.M. and B.Z. performed RNA-seq and related analyses. A.G.H., M.S.S., S.S.W., J.P., P.W., S.K.V., R.R.-A. and X.W. aided in experimental design and helped to interpret results. V.R.G., P.W., S.K.V., B.Z., F.J.B., T.C., R.A.F. and V.A.R. acquired the funding for this work. All authors reviewed and approved the manuscript.

**Competing interests** R.A.F. is a stockholder of ORNA Therapeutics. R.A.F. is a board of directors' member and stockholder of Chronus Health and Blue Planet Systems. V.R.G., R.A.F. and V.A.R. have filed a patent on the sequences and use of acp3U in various functional immune applications. The other authors declare no competing interests.

**Additional information**


**Supplementary information** The online version contains supplementary material available at https://doi.org/10.1038/s41586-025-09310-6.



**Correspondence and requests for materials** should be addressed to Ryan A. Flynn or Vijay A. Rathinam.



**Peer review information** *Nature* thanks Bryan Dickinson, Nan Yan and the other, anonymous, reviewer(s) for their contribution to the peer review of this work.

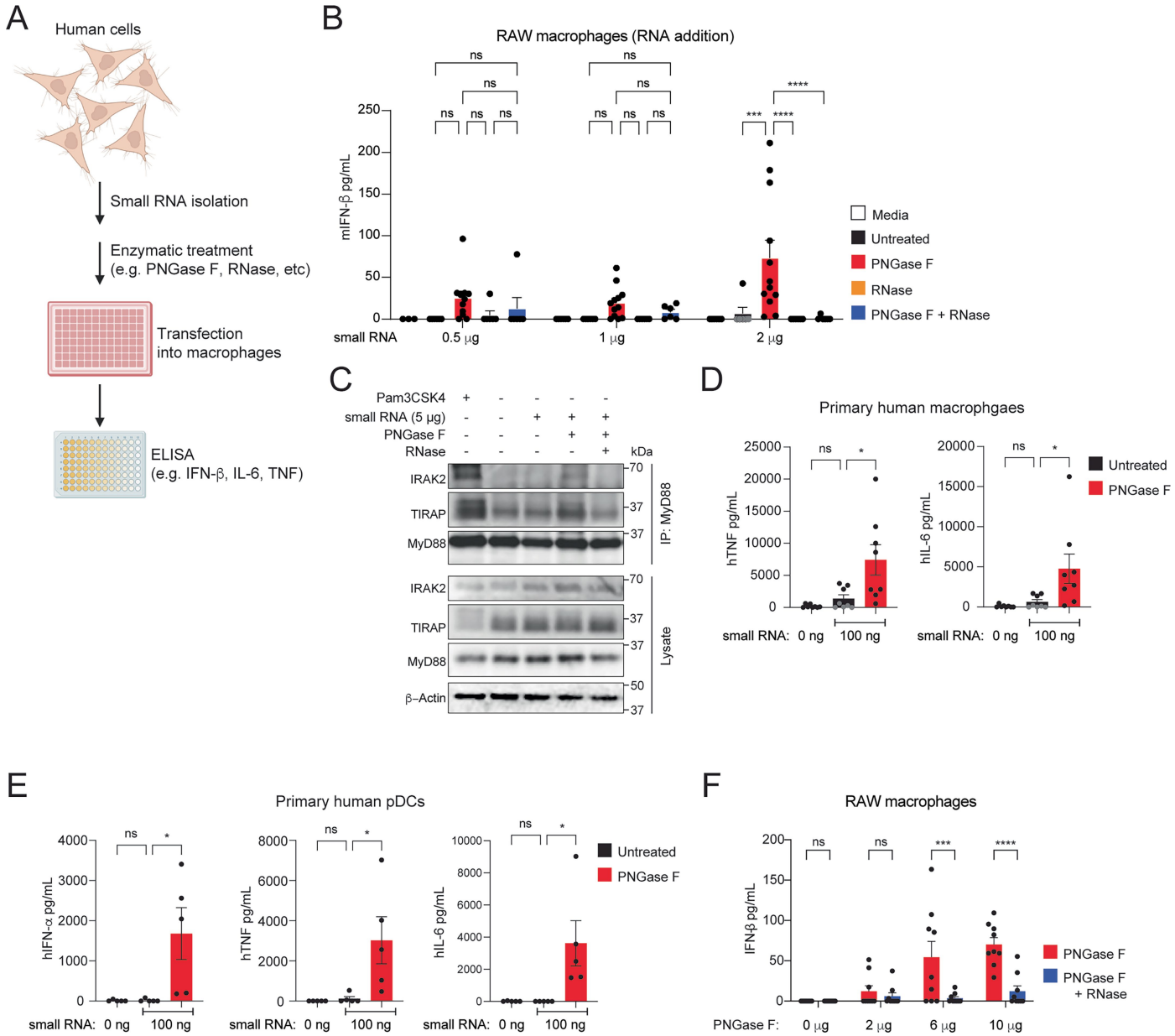


**Extended Data Fig. 1 | N-glycans shield small RNAs from innate immune recognition.** (**A**) Experimental design to test if the enzymatic removal of N-glycans from glycoRNAs induces a type I IFN response. (**B**) IFN-β ELISA of RAW macrophage supernatants 6 hours post-stimulation with 500 ng, 1 μg, or 2 μg of small RNAs untreated or treated with PNGase F, RNase cocktail, or PNGase F+RNase cocktail. (**C**) Immunoblotting for IRAK2, TIRAP and MyD88 in MyD88 immunoprecipitates and IRAK2, TIRAP, MyD88, and β-Actin in input lysates from macrophages stimulated as indicated. (**D**) TNF and IL-6 ELISA of supernatants from primary human macrophages stimulated with small RNAs treated with or without PNGase F (one dot = triplicate averages from one human donor). (**E**) IFN-α, TNF, IL-6 ELISA of supernatants from primary human plasmacytoid dendritic cells stimulated with small RNAs treated with or without PNGase F (one dot = triplicate averages from one human donor). (**F**) IFN-β ELISA of RAW macrophage supernatants 6 hours post treatment with 2 μg, 6 μg, or 10 μg of PNGase F alone or in combination with RNase. Pooled data from 3 (**F**) or 4 (**B, D, E**) independent experiments are shown as mean ± SEM (**B, D**–**F**) or one representative blot of two independent replicates (**C**). *, $p < 0.05$; ***, $p < 0.001$; ****, $p < 0.0001$; ns, not significant. Two-way ANOVA with Tukey's test (**B, F**), One-way ANOVA with Šídák's test (**D, E**). Schematic in **a** was created with BioRender (https://biorender.com).

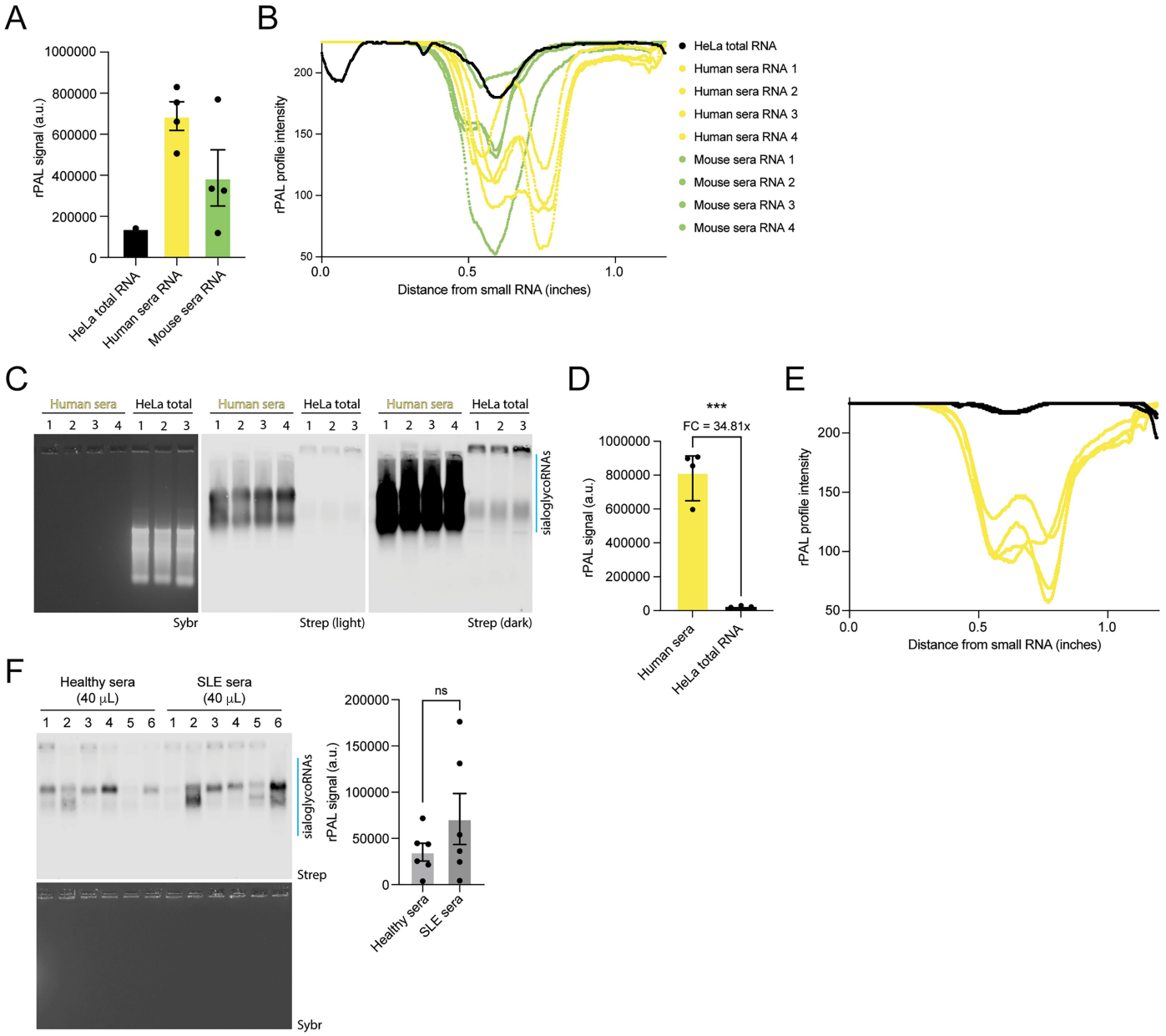


**Extended Data Fig. 2 | GlycoRNAs are present in the circulation.** (**A**) Quantification of rPAL signal from glycoRNAs enriched from human and mouse sera RNA. (**B**) One dot equals one donor/mouse. rPAL signal intensity of individual RNA samples (quantified in **A**). (**C**) Blotting of glycoRNAs from HeLa cells and human sera samples normalized at 1 µg of RNA per well. (**D**) Quantification of glycoRNA signal intensity observed in (**C**). (**E**) rPAL signal intensity of normalized human and HeLa cell-derived RNA samples (quantified in **D**). (**F**) Blotting of glycoRNAs from healthy human donors or SLE patient sera samples normalized at 1 µg of RNA per well. Data are represented as mean ± SEM (**A**, **C**, and **D**). Pooled data from four (**A**–**E**) or 6 (**F**) independent sera samples are shown. ***, $p < 0.001$; ns, not significant. Unpaired two-tailed t-test (**D**, **F**).

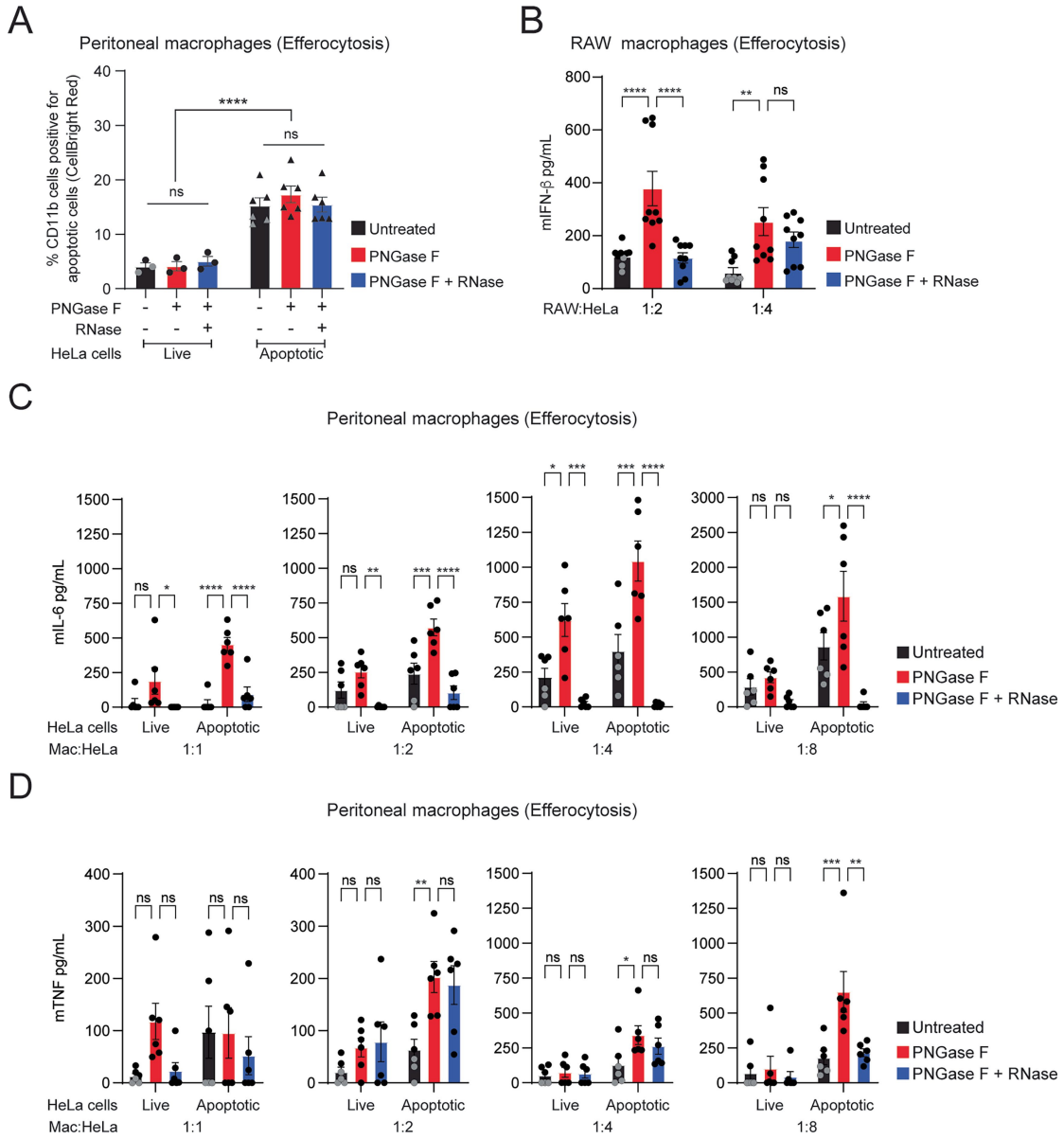


**Extended Data Fig. 3 | De-*N*-glycosylation of cell surface RNAs makes apoptotic cells immunostimulatory.** (**A**) Efferocytosis of CellBright Red-labeled live or apoptotic HeLa cells treated with or without PNGase F, or PNGase F+RNase cocktail by CD11b+ peritoneal macrophages 2 hours post-feeding as assessed via flow cytometry. (**B**) IFN-β ELISA of RAW macrophage supernatants 24 hours post-stimulation with apoptotic HeLa cells treated with or without PNGase F or PNGase F+RNase cocktail at indicated macrophage:HeLa cell ratios. (**C**) IL-6 ELISA of peritoneal macrophage supernatants 24 hours post-stimulation with live or apoptotic HeLa cells treated with or without PNGase F or PNGase F+RNase cocktail at indicated macrophage:HeLa cell ratios. (**D**) TNF ELISA of peritoneal macrophage supernatants 24 hours post-stimulation with live or apoptotic HeLa cells treated with or without PNGase F or PNGase F+RNase cocktail at indicated macrophage:HeLa cell ratios. Data are represented as mean ± SEM (**A**–**D**). Pooled data from 3 independent experiments (**A**–**D**) are shown. *, $p < 0.05$; **, $p < 0.01$; ***, $p < 0.001$; ****, $p < 0.0001$; ns, not significant. Two-way ANOVA with Tukey's test (**A**–**D**).

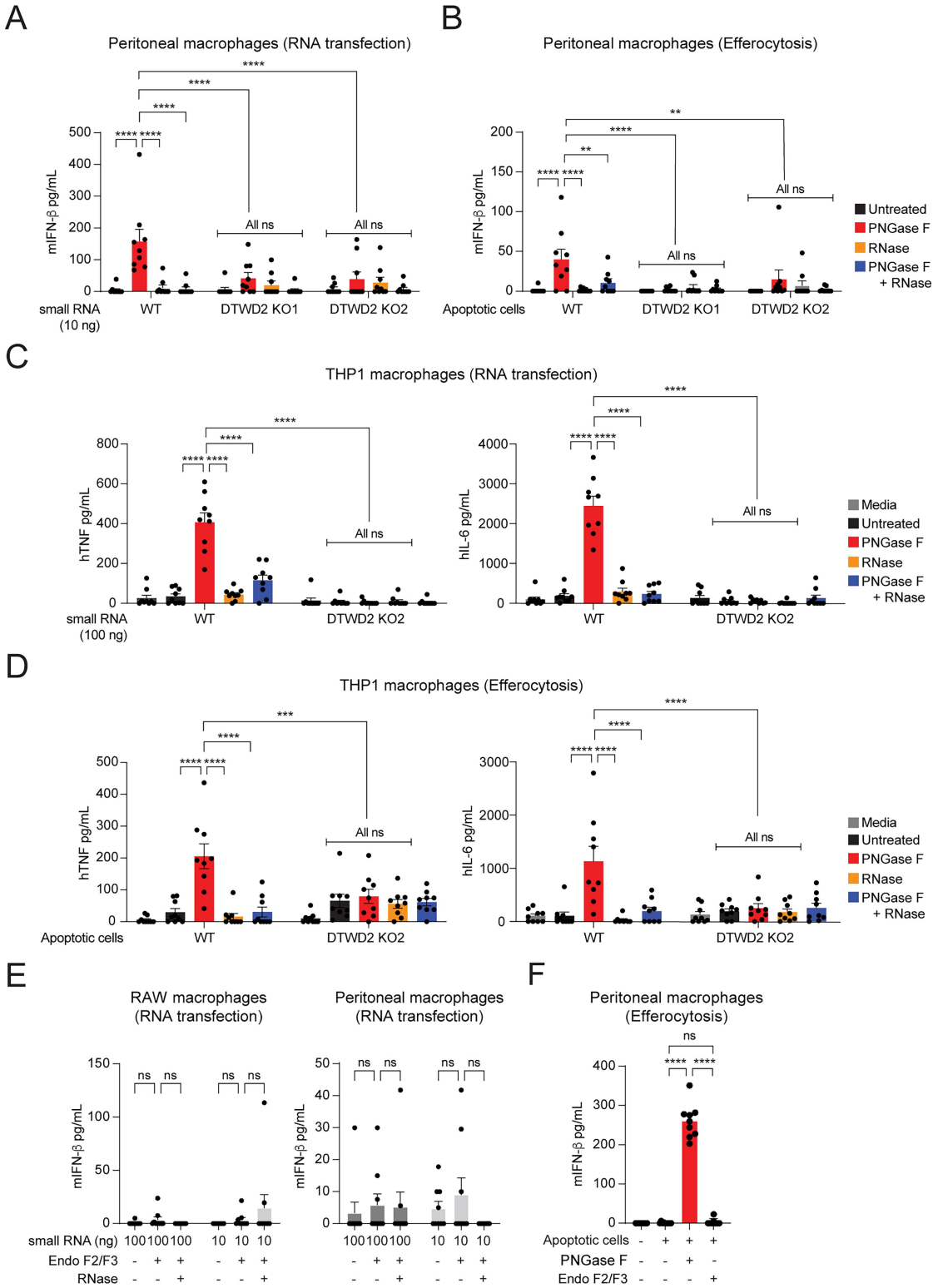


**Extended Data Fig. 4** | See next page for caption.

**Extended Data Fig. 4 | The modified RNA base acp$^3$U stimulates innate immune responses.** (**A**) IFN-β ELISA of peritoneal macrophage supernatants 6 hours post-transfection with small RNA derived from WT and two separate single cell clones of DTWD2 KO U2OS cells treated with or without PNGase F, RNase cocktail, or PNGase F+RNase cocktail. (**B**) IFN-β ELISA of peritoneal macrophage supernatants 24 hours post-stimulation with apoptotic WT, DTWD2 KO1 and DTWD2 KO2 U2OS cells treated with or without PNGase F or PNGase F with RNase cocktail at 1:2 macrophage:U2OS cell ratio. (**C**) TNF and IL-6 ELISAs of supernatants of THP1 macrophages 6 hours post-transfection of small RNAs harvested from DTWD2 KO cells treated with or without PNGase F or in combination with RNase. (**D**) TNF and IL-6 ELISAs of supernatants of THP1 macrophages 6 hours post-stimulation with apoptotic DTWD2 KO cells treated with or without PNGase F or in combination with RNase. (**E**) IFN-β ELISA of RAW macrophage (left panel) and peritoneal macrophage (right panel) supernatants 6 hours post-transfection with small RNA treated with or without Endo-F2/F3 or Endo-F2/F3+RNase cocktail (This experiment was performed at the same time as Fig. 1F). (**F**) IFN-β ELISA of peritoneal macrophage supernatants 24 hours post-stimulation with apoptotic HeLa cells treated with or without PNGase F or Endo-F2/F3 at 1:4 macrophage:HeLa cell ratio. Data are represented as mean ± SEM (**A**–**F**). Pooled data from 3 independent experiments (**A**–**F**) are shown. **, $p < 0.01$; ***, $p < 0.001$; ****, $p < 0.0001$; ns, not significant. Two-way ANOVA with Tukey's test (**A**–**E**) or One-way ANOVA with Šídák's test (**F**).

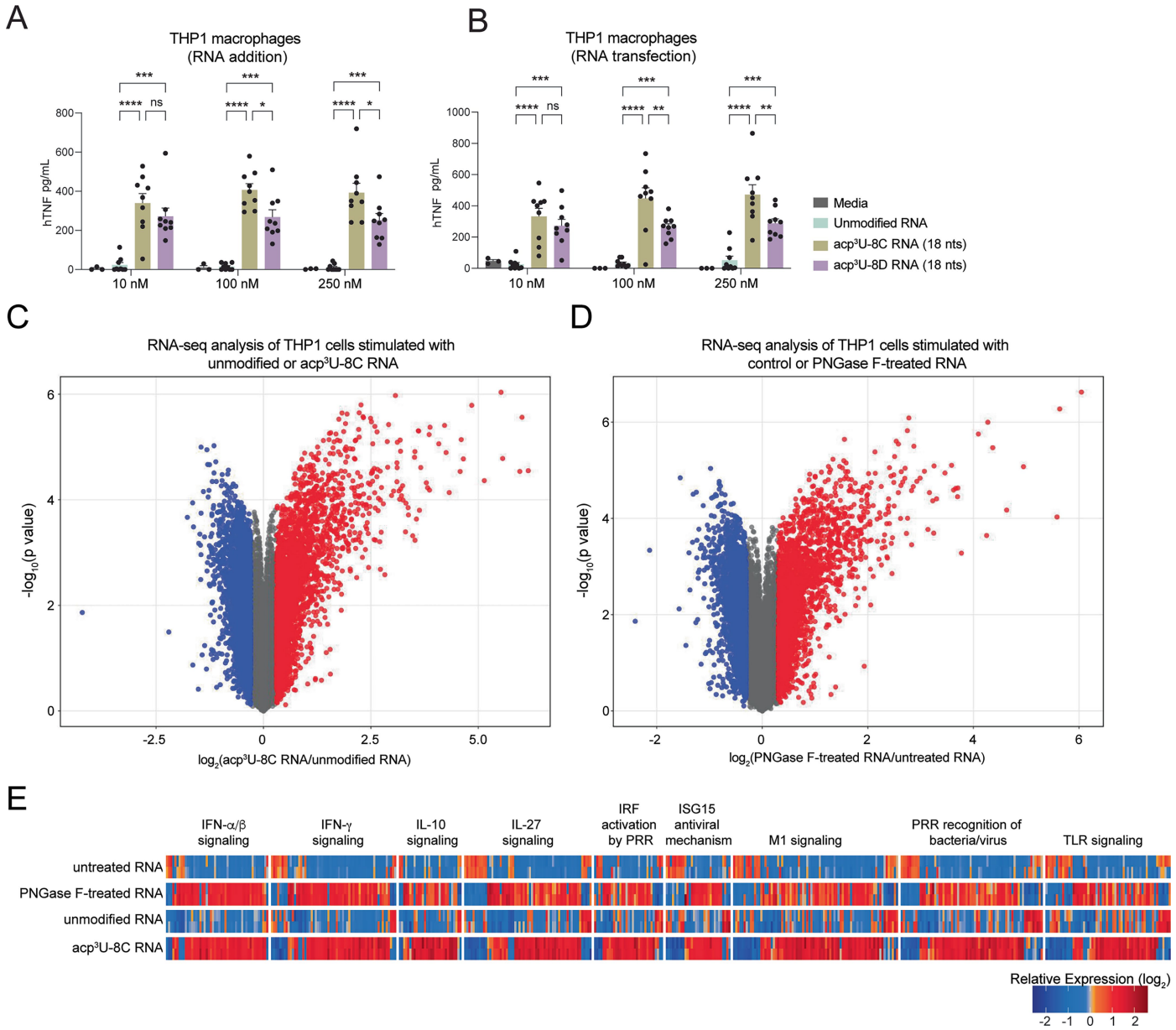


**Extended Data Fig. 5 | The modified RNA base acp$^3$U stimulates innate immune responses.** (**A** and **B**) TNF ELISA of THP-1 macrophage supernatants 6 hours post-stimulation (**A**) or post-transfection (**B**) with 10 nm, 100 nm, or 250 nm of synthetic unmodified RNA or synthetic RNA modified with acp$^3$U (acp$^3$U-8C and acp$^3$U-8D). (**C** and **D**) Volcano plot of differentially expressed genes in THP1 macrophages stimulated with acp$^3$U-8C-RNA (**C**) or PNGase F-treated small RNAs (**D**) compared to THP1 macrophages stimulated with unmodified RNA (**C**) or untreated small RNA (**D**), respectively, as revealed by RNA-seq. Each dot represents a gene (Total of 32,389 genes tested). A cutoff of absolute value fold-change of 0.5 was used to select significantly differentially expressed genes for gene ontology, yielding 5107 genes in PNGase F-treated small RNAs vs. untreated small RNAs and 6472 genes in acp$^3$U-8C RNA vs. unmodified RNA. (**E**) Heat map of the genes represented in the indicated immune pathways in THP1 macrophages stimulated as in **C** and **D**. Rows are samples grouped by condition; Columns are genes grouped by pathways; Color is the scaled expression of genes in each sample. Data are represented as mean ± SEM (**A** and **B**). Pooled data from 3 (**A** and **B**) or 2 (**C**–**E**) independent experiments are shown. *, $p < 0.05$; **, $p < 0.01$; ***, $p < 0.001$; ****, $p < 0.0001$; ns, not significant. Two-way ANOVA with Tukey's test (**A** and **B**).

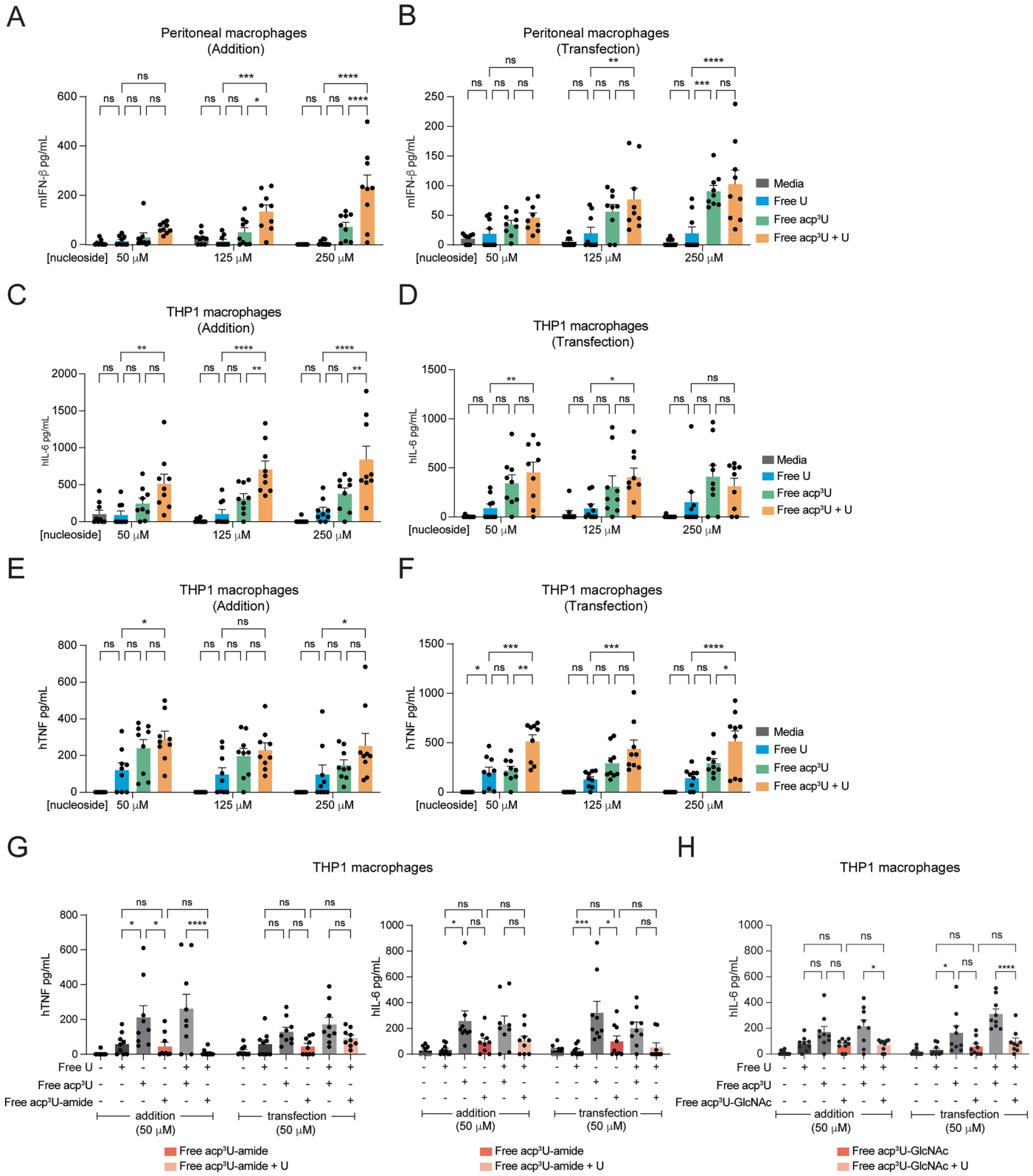


**Extended Data Fig. 6 | RNA with the modified base acp³U stimulates innate immune responses.** (**A** and **B**) IFN-β ELISA of peritoneal macrophage supernatants 6 hours post-stimulation (**A**) or post-transfection (**B**) with 50 μM, 125 μM, 250 μM of uridine, acp³U, or uridine+acp³U (**C** and **D**) IL-6 ELISA of THP-1 macrophage supernatant 6 hours post-stimulation (**C**) or post-transfection (**D**) with 50 μM, 125 μM, 250 μM of uridine, acp³U, or uridine+acp³U. (**E** and **F**) TNF ELISA of THP-1 macrophage supernatant 6 hours post-stimulation (**E**) or post-transfection (**F**) with 50 μM, 125 μM, 250 μM of uridine, acp³U, or uridine+acp³U. (**G**) IL-6 and TNF ELISA of THP-1 macrophage supernatant 6 hours post-addition or post-transfection with 50 μM of uridine, acp³U, acp³U-modified with an amide (acp³U amide), acp³U+uridine or acp³U amide+uridine. (**H**) IL-6 ELISA of THP-1 macrophage supernatant 6 hours post-addition or post-transfection with 50 μM of uridine, acp³U, acp³U-modified with a GlcNAc (acp³U-GlcNAc), acp³U+uridine or acp³U GlcNAc+uridine. Data are represented as mean ± SEM (**A**–**H**). Pooled data from 3 independent experiments (**A**–**H**) are shown. *, $p < 0.05$; **, $p < 0.01$; ***, $p < 0.001$; ****, $p < 0.0001$; ns, not significant. Two-way ANOVA with Tukey's test (**A**–**H**).

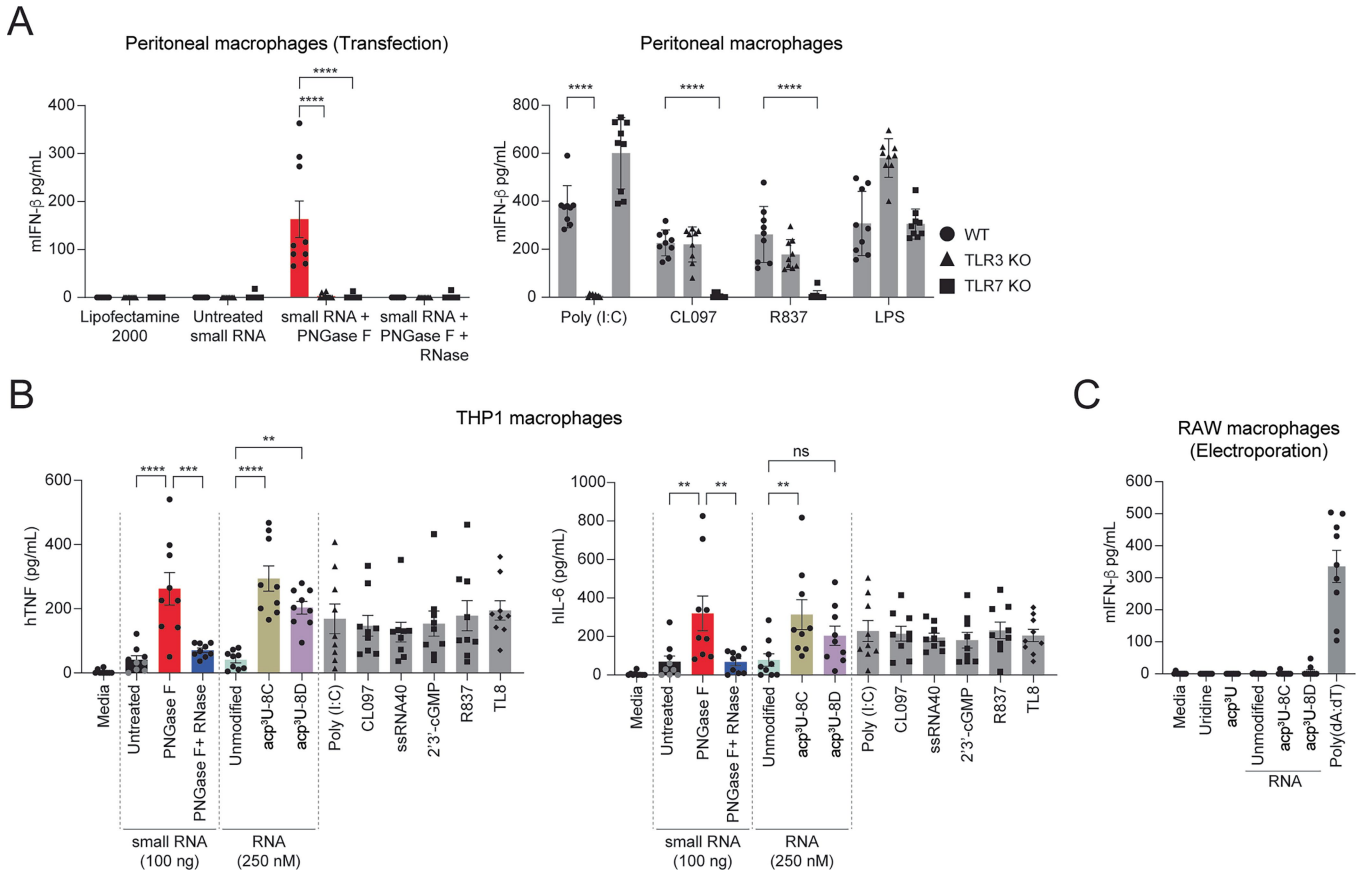


**Extended Data Fig. 7 | TLR3 and TLR7 sense de-*N*-glycosylated glycoRNAs.** (**A**) IFN-β ELISA of supernatants from WT, TLR3 KO, and TLR7 KO peritoneal macrophages stimulated for 24 hours with small RNAs from HeLa cells that were treated with or without PNGase F or in combination with RNase and then column purified to remove the associated N-glycans and enzymes. Poly(I:C), CL097, R837 and LPS were used as controls. (**B**) TNF and IL-6 ELISA of supernatants from THP1 macrophages stimulated with small RNAs treated with or without PNGase F, or in combination with RNase, unmodified or acp$^3$U-containing synthetic RNAs, as well as poly(I:C), CL097, ssRNA40, 2′,3′-cGMP, R837, and TL8. (**C**) IFN-β ELISA of supernatants of RAW macrophages 24 hours post-electroporation with free uridine, acp$^3$U, uridine+acp$^3$U in combination or the synthetic 18-nucleotide unmodified or acp$^3$U containing RNAs and poly(dA:dT). Pooled data from 3 independent experiments (**A**–**C**) are shown. **, $p < 0.01$; ***, $p < 0.001$; ****, $p < 0.0001$; ns, not significant. Two-way ANOVA with Tukey's test (**A**) or One-way ANOVA with Šídák's test (**B**–**C**).

nature portfolio

Corresponding author(s): Ryan Flynn
Vijay Rathinam

Last updated by author(s): Jun 15, 2024

# Reporting Summary

Nature Portfolio wishes to improve the reproducibility of the work that we publish. This form provides structure for consistency and transparency in reporting. For further information on Nature Portfolio policies, see our Editorial Policies and the Editorial Policy Checklist.

## Statistics

For all statistical analyses, confirm that the following items are present in the figure legend, table legend, main text, or Methods section.

| n/a | Confirmed |
|---|---|
| ☐ | ☒ The exact sample size (*n*) for each experimental group/condition, given as a discrete number and unit of measurement |
| ☐ | ☒ A statement on whether measurements were taken from distinct samples or whether the same sample was measured repeatedly |
| ☐ | ☒ The statistical test(s) used AND whether they are one- or two-sided<br>*Only common tests should be described solely by name; describe more complex techniques in the Methods section.* |
| ☒ | ☐ A description of all covariates tested |
| ☒ | ☐ A description of any assumptions or corrections, such as tests of normality and adjustment for multiple comparisons |
| ☐ | ☒ A full description of the statistical parameters including central tendency (e.g. means) or other basic estimates (e.g. regression coefficient) AND variation (e.g. standard deviation) or associated estimates of uncertainty (e.g. confidence intervals) |
| ☐ | ☒ For null hypothesis testing, the test statistic (e.g. *F*, *t*, *r*) with confidence intervals, effect sizes, degrees of freedom and *P* value noted<br>*Give P values as exact values whenever suitable.* |
| ☒ | ☐ For Bayesian analysis, information on the choice of priors and Markov chain Monte Carlo settings |
| ☐ | ☒ For hierarchical and complex designs, identification of the appropriate level for tests and full reporting of outcomes |
| ☒ | ☐ Estimates of effect sizes (e.g. Cohen's *d*, Pearson's *r*), indicating how they were calculated |

*Our web collection on statistics for biologists contains articles on many of the points above.*

## Software and code

Policy information about availability of computer code

| | |
|---|---|
| Data collection | FACSymphonyTM A5 (BD Biosciences), BMG Labtech CLARIOstar, Azure 600. |
| Data analysis | Statistical analysis was performed in GraphPad PRISM v10.1.2 unpaired t-test or one-way or two-way ANOVA as indicated in the figure legends, and Microsoft excel 2016. RNA-seq data analyses were conducted with R v4.4.0. |

For manuscripts utilizing custom algorithms or software that are central to the research but not yet described in published literature, software must be made available to editors and reviewers. We strongly encourage code deposition in a community repository (e.g. GitHub). See the Nature Portfolio guidelines for submitting code & software for further information.

## Data

Policy information about availability of data

All manuscripts must include a data availability statement. This statement should provide the following information, where applicable:

- Accession codes, unique identifiers, or web links for publicly available datasets
- A description of any restrictions on data availability
- For clinical datasets or third party data, please ensure that the statement adheres to our policy

RNAseq datasets deposited under GEO accession no. GSE291767.

## Research involving human participants, their data, or biological material

Policy information about studies with human participants or human data. See also policy information about sex, gender (identity/presentation), and sexual orientation and race, ethnicity and racism.

| | |
|---|---|
| Reporting on sex and gender | N/A |
| Reporting on race, ethnicity, or other socially relevant groupings | N/A |
| Population characteristics | N/A |
| Recruitment | N/A |
| Ethics oversight | N/A |

Note that full information on the approval of the study protocol must also be provided in the manuscript.

# Field-specific reporting

Please select the one below that is the best fit for your research. If you are not sure, read the appropriate sections before making your selection.

☒ Life sciences ☐ Behavioural & social sciences ☐ Ecological, evolutionary & environmental sciences

For a reference copy of the document with all sections, see nature.com/documents/nr-reporting-summary-flat.pdf

# Life sciences study design

All studies must disclose on these points even when the disclosure is negative.

| | |
|---|---|
| Sample size | No statistical methods were used to determine the sample size. Sample sizes were determined based on optimization experiments, previous experience, and our published literature on the subject area (Vasudevan et al., Cell Reports 2022 PMID: 35508125; Kumari et al., Cell Reports 2021 PMID:33882312) which suggested that chosen sample size is adequate for the study. For glycoRNA blotting, we performed rPAL analysis with 4-6 independent samples from different donors to show variability across different samples at the input quantity of 1 ug of RNA as described in Flynn et al., 2021. |
| Data exclusions | No data was excluded in this study. |
| Replication | All experiments were performed at least two or three times as independent experiments and were successfully replicated. This is indicated in the figure legends for each experiments. |
| Randomization | No randomization was performed in this study. Sex- and age-matched mice were assigned to different experimental groups. |
| Blinding | No blinding was performed in this study. All results and analysis were based on objective quantification of the data collected through automated instrumentation. |

# Reporting for specific materials, systems and methods

We require information from authors about some types of materials, experimental systems and methods used in many studies. Here, indicate whether each material, system or method listed is relevant to your study. If you are not sure if a list item applies to your research, read the appropriate section before selecting a response.

### Materials & experimental systems

| n/a | Involved in the study |
|---|---|
| ☐ | ☒ Antibodies |
| ☐ | ☒ Eukaryotic cell lines |
| ☒ | ☐ Palaeontology and archaeology |
| ☐ | ☒ Animals and other organisms |
| ☒ | ☐ Clinical data |
| ☒ | ☐ Dual use research of concern |
| ☒ | ☐ Plants |

### Methods

| n/a | Involved in the study |
|---|---|
| ☒ | ☐ ChIP-seq |
| ☒ | ☐ Flow cytometry |
| ☒ | ☐ MRI-based neuroimaging |

## Antibodies

Antibodies used

All antibodies used in this study are commercially available and used extensively. These antibodies and their clones names/CAT# are included in the methods section of this manuscript.
Coating antibody: anti-mIFN-β monoclonal antibody sc-57201, Santa Cruz Biotechnology: https://www.scbt.com/p/ifn-beta-antibody-7f-d3
Detection mIFN-β antibody 32400-1, PBL Assay Science: https://www.pblassaysci.com/antibodies/anti-mouse-ifn-beta-antibody-rabbit-serum-neutralizing-pab-32400
phospho-IRF3 (1:1000 dilution, 4D4G, 4947, Cell Signaling Technology): https://www.cellsignal.com/products/primary-antibodies/phospho-irf-3-ser396-4d4g-rabbit-mab/4947
phospho-TBK1 (1:1000 dilution, 5483, D52C2, Cell Signaling Technology): https://www.cellsignal.com/products/primary-antibodies/phospho-tbk1-nak-ser172-d52c2-xp-rabbit-mab/5483
phospho-ERK1/2 (1:1000 dilution, 9106, (Thr202/Tyr204), Cell Signaling Technology): https://www.cellsignal.com/products/primary-antibodies/phospho-p44-42-mapk-erk1-2-thr202-tyr204-e10-mouse-mab/9106
phospho-JNK (1:1000 dilution, 9251 (Thr183/Tyr185), Cell Signaling Technology): https://www.cellsignal.com/products/primary-antibodies/phospho-sapk-jnk-thr183-tyr185-antibody/9251
phospho-p65 (1:1000 dilution, 3031, (Ser536), Cell Signaling Technology): https://www.cellsignal.com/products/primary-antibodies/phospho-nf-kb-p65-ser536-antibody/3031
phospho-p38 (1:1000 dilution, 4511 (Thr180/Tyr182, D3F9), Cell Signaling Technology): https://www.cellsignal.com/products/primary-antibodies/phospho-p38-mapk-thr180-tyr182-d3f9-xp-rabbit-mab/4511
total IRF3 (1:1000 dilution, 4302, D83B9, Cell Signaling Technology): https://www.cellsignal.com/products/primary-antibodies/irf-3-d83b9-rabbit-mab/4302
total TBK1 (1:1000 dilution, 51872, E9H5S, Cell Signaling Technology): https://www.cellsignal.com/products/primary-antibodies/tbk1-nak-e9h5s-mouse-mab/51872
total ERK1/2 (1:1000 dilution, 9102, Cell Signaling Technology):https://www.cellsignal.com/products/primary-antibodies/p44-42-mapk-erk1-2-antibody/9102
total JNK (1:1000 dilution, 9252, Cell Signaling Technology): https://www.cellsignal.com/products/primary-antibodies/sapk-jnk-antibody/9252
total p65 (1:1000 dilution, 6956, (L8F6), Cell Signaling Technology): https://www.cellsignal.com/products/primary-antibodies/nf-kb-p65-l8f6-mouse-mab/6956
total p38 (1:1000 dilution, 8690, (D13E1), Cell Signaling Technology): https://www.cellsignal.com/products/primary-antibodies/p38-mapk-d13e1-xp-rabbit-mab/8690
α-Tubulin (1:1000 dilution, 3873, DM1A, Cell Signaling Technology): https://www.cellsignal.com/products/primary-antibodies/a-tubulin-dm1a-mouse-mab/3873
β-Actin, (1:1000, 3700, (8H10D10), Cell signaling technology): https://www.cellsignal.com/products/primary-antibodies/b-actin-8h10d10-mouse-mab/3700
HRP-conjugated anti-rabbit (1:5000 dilution, 711035152, Jackson ImmunoResearch): https://www.jacksonimmuno.com/catalog/products/711-035-152
HRP-conjugated anti-mouse (1:5000 dilution, 115035166, Jackson ImmunoResearch): https://www.jacksonimmuno.com/catalog/products/115-035-166
HRP-conjugated anti-goat (1:5000 dilution, 805035180, Jackson ImmunoResearch): https://www.jacksonimmuno.com/catalog/products/805-035-180
CD11b antibody (catalogue no: 101211; Biolegend): https://www.biolegend.com/ja-jp/products/apc-anti-mouse-human-cd11b-antibody-345
Streptavidin IR800 (1:5000 dilution, LiCor Biosciences, 926-32230): https://shop.licor.com/bio/reagents/irdye-800cw-streptavidin
MyD88 (1:1000 dilution, AF3109, R&D systems): https://www.rndsystems.com/products/mouse-rat-myd88-antibody_af3109
TIRAP (1:1000 dilution, 13077T, Cell Signaling Technologies): https://www.cellsignal.com/products/primary-antibodies/tirap-d6m9z-rabbit-mab/13077
IRAK2 (1:1000 dilution, 4367T, Cell Signaling Technologies): https://www.cellsignal.com/products/primary-antibodies/irak2-antibody/4367

Validation

All antibodies are commercially available and validated by the manufacturer on their websites. We selected the antibodies used in this study due to the validation provided by each manufacturer for their use in immunoblotting and co-immunopreciptation. Details on these antibody validation can be used by search the manufacturer's website using the information provided above.

## Eukaryotic cell lines

Policy information about cell lines and Sex and Gender in Research

Cell line source(s)

HeLa, ATCC
RAW264.7 macrophages ATCC ATCC TIB-71
THP1 cells ATCC, provided by Dr. Kate Fitzgerald's UMass Chan Medical School
U20S cells, ATCC
DTWD2 KO cells were generated in the Flynn lab and validated in their manuscript (PMID: 39173631).

Authentication

The cell lines were authenticated from the manufacturer. No futher validation was performed in lab.

Mycoplasma contamination

Cell lines were not tested for Mycoplasma in the lab.

Commonly misidentified lines
(See ICLAC register)

No misidentified cell lines were used.

## Animals and other research organisms

Policy information about studies involving animals; ARRIVE guidelines recommended for reporting animal research, and Sex and Gender in Research

| | |
|---|---|
| Laboratory animals | Wild-type (WT) C57BL/6J, TLR3 KO (Strain B6;129S1-Tlr3tm1Flv/J), TLR7 KO (Strain B6.129S1-Tlr7tm1Flv/J), MyD88 KO (Strain B6.129P2(SJL)-Myd88/J) and TRIF KO (Strain C57BL/6J-Ticam1/J) from the Jackson laboratory (Bar harbor, ME) were bred and maintained in specific pathogen-free conditions in the animal facility of UConn Health. All mice were housed at an ambient temperature of approximately 22 °C, a humidity of 40–60%, and a light/dark cycle of 12 hours. Sex- and age-matched mice were used. All mice used in this study were between the age of 6-20 weeks old. |
| Wild animals | The study did not involve wild animals. |
| Reporting on sex | Findings are applicable to male and female mice. |
| Field-collected samples | The study did not involve samples collected from the field. |
| Ethics oversight | The animal studies were approved by the UConn Health Institutional Animal Care and Use Committee (IACUC) |

Note that full information on the approval of the study protocol must also be provided in the manuscript.

## Plants

| | |
|---|---|
| Seed stocks | N/A |
| Novel plant genotypes | N/A |
| Authentication | N/A |